OXFORD GENETICS

GENETICS, 2023, 225(2), iyad144
https://doi.org/10.1093/genetics/iyad144
Advance Access Publication Date: 2 August 2023
Investigation

Hyperactive Ras disrupts cell size control and a key step in cell cycle entry in budding yeast

Jerry T. DeWitt, Jennifer C. Chinwuba, Douglas R. Kellogg*

Department of Molecular, Cell and Developmental Biology, University of California, Santa Cruz, CA 95064, USA

*Corresponding author: Department of Molecular, Cell and Developmental Biology, University of California, Santa Cruz, 1156 High Street Santa Cruz, CA 95064, USA. Email: dkellogg@ucsc.edu

Abstract

Severe defects in cell size are a nearly universal feature of cancer cells. However, the underlying causes are unknown. A previous study suggested that a hyperactive mutant of yeast Ras (*ras2*^{G19V}) that is analogous to the human Ras oncogene causes cell size defects, which could provide clues to how oncogenes influence cell size. However, the mechanisms by which *ras2*^{G19V} influences cell size are unknown. Here, we found that *ras2*^{G19V} inhibits a critical step in cell cycle entry, in which an early G1 phase cyclin induces transcription of late G1 phase cyclins. Thus, *ras2*^{G19V} drives overexpression of the early G1 phase cyclin Cln3, yet Cln3 fails to induce normal transcription of late G1 phase cyclins, leading to delayed cell cycle entry and increased cell size. *ras2*^{G19V} influences transcription of late G1 phase cyclins via a poorly understood step in which Cln3 inactivates the Whi5 transcriptional repressor. Previous studies found that yeast Ras relays signals via protein kinase A (PKA); however, *ras2*^{G19V} appears to influence *late* G1 phase cyclin expression via novel PKA-independent signaling mechanisms. Together, the data define new mechanisms by which hyperactive Ras influences cell cycle entry and cell size in yeast. Hyperactive Ras also influences expression of G1 phase cyclins in mammalian cells, but the mechanisms remain unclear. Further analysis of Ras signaling in yeast could lead to discovery of new mechanisms by which Ras family members control expression of G1 phase cyclins.

Keywords: Ras; G1 phase; cyclin; cell cycle; cell size; yeast; cell cycle entry; Cln3; Cln2; oncogene

Introduction

Cells within the human body range in size over several orders of magnitude. However, cells of a particular type maintain a constant average size. Thus, cell growth must be tightly controlled to ensure that cells attain and maintain an appropriate cell size (Jorgensen and Tyers 2004; Turner *et al.* 2012; Liu *et al.* 2022). At the simplest level, the size and shape of a cell must be the outcome of conserved mechanisms that determine the extent, location, and timing of cell growth. In dividing cells, maintenance of a specific cell size is ensured by mechanisms that link cell cycle progression to cell growth. These mechanisms are modulated by nutrients such that the threshold amount of growth required for cell cycle progression is reduced in poor nutrients, which leads to a reduction in cell size (Kellogg and Levin 2022). The mechanisms that control cell growth and size remain poorly understood.

Previous studies in budding yeast suggested that a Ras signaling network is required for normal control of cell size. Yeast Ras is encoded by a pair of redundant paralogs referred to as RAS1 and RAS2. Cells lacking either paralog are viable but loss of both is lethal (Toda *et al.* 1985). The functions of yeast Ras are best understood in the context of a signaling network that is activated by glucose. High glucose activates Ras, which then activates adenylate cyclase to produce cAMP. The cAMP binds Bcy1, an inhibitory subunit for cAMP-dependent protein kinase (PKA) (Matsumoto *et al.* 1983; Toda *et al.* 1987). Binding of cAMP to Bcy1 causes it to dissociate from PKA, leading to release of active PKA that initiates a signaling network with pervasive effects on control of cell growth and metabolism (Robinson *et al.* 1987; Zaman *et al.* 2009). A hyperactive allele of RAS2 (*ras2*^{G19V}) that is analogous to oncogenic alleles of mammalian Ras was found to cause an increase in cell size in diploid cells that also contain a mutant allele of CDC25, which is the budding yeast Ras-GEF (Broek *et al.* 1987; Baroni *et al.* 1989). However, the effects of hyperactive *ras2*^{G19V} on cell size have not been tested in a wildtype background. Deletion of *IRA2*, a budding yeast Ras-GAP that is conserved in mammals, also causes an increase in cell size (Jorgensen *et al.* 2002). Furthermore, a weakly constitutive allele of PKA in a *bcy1*Δ background causes a failure in nutrient modulation of cell size (Tokiwa *et al.* 1994). Together, these observations suggest that a Ras–PKA signaling axis influences cell size and plays a role in nutrient modulation of cell size; however, the mechanisms are poorly understood. Furthermore, little is known about yeast Ras signaling beyond the PKA pathway, and it remains possible that Ras influences cell size via signaling pathways that are distinct from the canonical Ras–PKA pathway.

Ras proteins are highly conserved, and mammalian Ras homologs serve as master regulators of growth, proliferation, metabolism, and survival (Cazzanelli *et al.* 2018; Weiss 2020). Ras family members are amongst the most frequently mutated oncogenic drivers; it is thought that between 25% and 30% of all human cancers have oncogenic mutations in 1 or more Ras genes (Hobbs *et al.* 2016). A potential role for Ras family members in controlling cell

Received: June 08, 2023. **Accepted:** July 15, 2023

size is intriguing, since severe defects in cell size homeostasis are broadly linked to cancer (Brimo *et al.* 2013; Hoda *et al.* 2018; Asa 2019; Asadullah *et al.* 2021; Gothwal *et al.* 2021; Sandlin *et al.* 2022). For example, most cancers are associated with greater heterogeneity of cell size and shape, as well as dramatically altered nuclear-to-cytoplasmic volume ratios. Defects in cell size and shape have long been used by pathologists to diagnose cancer, and increased heterogeneity of cell size is associated with poor prognosis (Asadullah *et al.* 2021). The size defects of cancer cells must be caused, either directly or indirectly, by oncogenic signals. However, the mechanisms by which oncogenic signals influence cell growth and size are largely unknown, and it is unclear whether the size defects of cancer cells are a direct consequence of primary oncogenic signals or a secondary consequence of mutations that accumulate during evolution of cancer cells. The fact that diverse cancers show common defects in cell size suggests the possibility that diverse oncogenic signals converge on common conserved pathways for cell size control.

Since it is unknown how oncogenic signals influence cell size in human cells, or how hyperactive Ras influences cell size in yeast, it is possible that oncogenic Ras influences cell size via mechanisms that are conserved from yeast to humans. Thus, the analysis of how hyperactive Ras influences cell size in yeast could provide new clues to the functions of oncogenic Ras in human cells. Here, we carried out new analyses of the effects of constitutively active Ras in budding yeast, utilizing modern methods that allow rapid inducible expression of *ras2*^{G19V} at endogenous levels in otherwise wildtype cells, which allowed us to discern the immediate consequences of *ras2*^{G19V} activity during the cell cycle. We found that *ras2*^{G19V} strongly influences expression of both early and late G1 phase cyclins, and that *ras2*^{G19V} disrupts a key step in which early G1 phase cyclins induce expression of late G1 phase cyclins. The effects of hyperactive Ras on late G1 phase cyclins are potentially mediated via signaling mechanisms that are independent of the canonical Ras–PKA signaling axis. Ras also influences expression of G1 phase cyclins in mammalian cells, potentially via signaling mechanisms that are distinct from the canonical MAP kinase pathway that is downstream of Ras (Kerkhoff and Rapp 1998; Muise-Helmericks *et al.* 1998; Pruitt *et al.* 2000; Pruitt and Der 2001; Coleman *et al.* 2004). Together, these observations suggest that much remains to be learned about how Ras family members influence G1 phase cyclin expression, cell cycle entry, and cell size.

Materials and methods

Yeast strains, plasmids, and media

The genotypes of the strains used in this study are listed in Table 1. All strains are in the W303 background (*leu2-3,112 ura3-1 can1-100 ade2-1 his3-11,15 trp1-1 GAL+, ssd1-d2*). Genetic alterations, such as addition of epitope tags, promoter swaps, and gene deletions, were carried out using homologous recombination at the endogenous locus (Longtine *et al.* 1998; Janke *et al.* 2004). Strains that express *RAS2* or *ras2*^{G19V} from the estradiol-inducible lexA promoter at the *RAS2* locus were generated by homologous recombination as previously described (Ottoz *et al.* 2014). Briefly, *lexA* promoter elements were amplified and integrated upstream of the wildtype *RAS2* locus (oligos: *TAACCGTTTTCGAATTGAAAGG AGATATACAGAAAAAAAACGAGAGCTTGCCTTGTCCCC* and *GTA CTCTCTTATGTTCGACTTGTTCAAAGGCATAAGCTTGATATCGAAT-TCCTG*). To create the *ras2*^{G19V} allele, the *ras2*^{G19V} mutation was incorporated into the 3′ oligo (oligo: *ATTGGGTCAATTGTATGGTCA AAGCAGATTTACCAACACCAACACCACCAACGACGACTAGCTTGT ACTCTCTTATGTTCGACTTGTTCAAAGGCATAAGCTTGATATCGAAT TCCTG*). The *ras2*^{G19V} mutant was verified by sequencing.

A plasmid (pJTD14A) that allows for integration of a wildtype copy of the *RAS2* gene at the *URA3* locus was created by amplifying the *RAS2* locus with approximately 200-bp upstream and downstream of the *RAS2* coding sequence (oligos: CCCGAATT CCCTAGAATCGC-TCATTTCAAG and CCCAAGCTTGCAACCAT ATGATATTGCCC) and then cloning into the EcoR1 and HindIII sites of YIPlac211. The plasmid is cut with StuI to target integration at *URA3*.

Cells were grown in YP medium (1% yeast extract, 2% peptone) that contained 40-mg/L adenine and a carbon source. Rich carbon medium (YPD) contained 2% dextrose, while poor carbon medium (YPG/E) contained 2% glycerol and 2% ethanol. In experiments using the ATP analog inhibitors 1-NM-PP1 or 3-MOB-PP1, no additional adenine was added to the media. All ATP analog inhibitors were solubilized in 100% DMSO. 3-MOB-PP1 was a gift from Kevin Shokat (UCSF). β-Estradiol (#50-28-2 from Acros) was added to cultures from a 10-mM stock in 100% ethanol.

Cell cycle time-courses and serial dilution assays

Cell cycle time courses were carried out as previously described (Harvey *et al.* 2011). Briefly, cells were grown to log phase at room temperature overnight in YPD or YPG/E medium to an optical density (OD^{600}) of 0.5–0.7. Cultures were adjusted to the same optical density and were then arrested in G1 phase with alpha factor at room temperature for 3 hours. *bar1* strains were arrested with 0.5-μg/mL alpha factor, while *BAR1*+ strains were arrested with 15-μg/mL alpha factor. Cells were released from the arrest by washing 3 times with YPD or YPG/E. All time courses were carried out at 30°C unless otherwise noted, and alpha factor was added back at 40 minutes to prevent initiation of a second cell cycle. For experiments involving induced expression of *RAS2* or *ras2*^{G19V}, cells were arrested for 3 hours and β-estradiol (200 nM) was added 1.5 hours before release. Cells were released from the arrest by washing 3 times with fresh YPD containing 200-nM β-estradiol.

Serial dilution assays were carried out by growing cells overnight in YPD to an OD^{600} of 0.4. A series of 10-fold dilutions were prepared, spotted on YPD plates, and grown for 2 days at 30°C.

Northern blotting

Gel-purified PCR products were used to generate radio-labeled probes to detect *CLN2* and *ACT1* mRNAs by northern blotting (*CLN2* oligonucleotides: TCAAGTTGGATGCAATTTGCAG, *TGAAC CAATGATCAATGATTACGT*; *ACT1* oligonucleotides: TCATACCT TCTACAACGA-ATTGAGA and ACACTTCATGATGGAGTTGT AAGT). Probes were labeled using the Megaprime DNA labeling kit (GE Healthcare). Northern blotting was carried out as previously described (*Cross and Tinkelenberg* 1991; *Kellogg and Murray* 1991). *CLN3* blots were stripped and reprobed for *ACT1* to control for loading.

ChIP and qPCR

ChIPs were performed as previously described (*Wang et al.* 2009). Yeast cells were collected at an OD of 0.6–0.8 and cross-linked in 1% formaldehyde for 15 minutes at room temperature. Cross-linking was quenched with 0.125-M glycine for 5 minutes, and cells were washed twice with 1× TBS (0.05-M Tris, 0.15-M NaCl, pH 7.6). Cell pellets were resuspended in lysis buffer (0.1% deoxycholic acid, 1-mM EDTA, 50-mM HEPES, pH 7.5, 140-mM NaCl, 1% Triton X-100 supplemented with protease inhibitors) and were lysed with 0.5-mm glass beads (BioSpec #11079105) in a cell disrupter (Mini-Beadbeater; BioSpec). After centrifugation, the pellet was washed with lysis buffer and sonicated to a shearing size of <500 nucleotides using a bath sonicator (Biorupter XL;

Table 1. List of budding yeast strains used in this study.

Strain	Genotype	Source	Figures
DK4040	*MATa bar1 ras2Δ::URA3*	This study	Fig. 1
DK4042	*MATa bar1 ras1Δ::KANMX*	This study	Fig. 1 and Supplementary Fig. 1b
DK4064	*MATa bar1 ras2^{G19V}*	This study	Fig. 1 and Supplementary Fig. 1a
DK4099	*MATa bar1 ras1Δ::KANMX ras2^{G19V}*	This study	Supplementary Fig. 1a
DK4333	*MATa bar1 ira2ΔirKANMX*	This study	Fig. 1
DK4426	*MATa bar1 LexA-ER-B112::HIS3*	This study	Figs. 2, 3, and 5
DK4450	*MATa bar1 LexA-ER-B112::HIS3 HPHNT1::(2x)lexA-RAS2*	This study	Figs. 2 and 3
DK4452	*MATa bar1 LexA-ER-B112::HIS3 HPHNT1::(2x) lexA-ras2^{G19V}*	This study	Figs. 2, 3, and 5
DK4495	*MATa bar1 LexA-ER-B112::HIS3 CLN3-6xHA::NATNT2 CLN2-13xMYC::KANMX*	This study	Fig. 3, Supplementary Fig. 2a, Fig. 7, Supplementary Fig. 4a, and Fig. 8
DK4496	*MATa bar1 LexA-ER-B112::HIS3 HPHNT1::(2x) lexA-RAS2 CLN3-6xHA::NATNT2 CLN2-13xMYC::KANMX*	This study	Fig. 3 and Supplementary Fig. 2a
DK4497	*MATa bar1 LexA-ER-B112::HIS3 HPHNT1::(2x) lexA-ras2^{G19V} CLN3-6xHA::NATNT2 CLN2-13xMYC::KANMX*	This study	Fig. 3, Supplementary Fig. 2a, Fig. 7, Supplementary Fig. 4a–b, and Fig. 8
DK4518	*MATa bar1 CLN3-6xHA::NATNT2 CLN2-13xMYC::KANMX whi3Δ::URA3*	This study	Fig. 7 and Supplementary Fig. 4a
DK4519	*MATa, bar1, LexA-ER-B112::HIS3, HPHNT1::(2x) lexA-ras2^{G19V} CLN3-6xHA::NATNT2, CLN2-13xMYC::KANMX whi3Δ::URA3*	This study	Fig. 7 and Supplementary Fig. 4a
DK4580	*MATa bar1 LexA-ER-B112::HIS3 HPHNT1::(2x) lexA-ras2^{G19V} CLN2-9xMYC::NATNT2*	This study	Fig. 5
DK4589	*MATa bar1 CLN3-6xHA::HIS3 KANMX::Gal-CLN2*	This study	Fig. 9
DK4597	*MATa bar1 LexA-ER-B112::HIS3 HPHNT1::(2x) lexA-ras2^{G19V} KANMX::MET25-CLN2-9xMYC::NATNT2*	This study	Fig. 5
DK4629	*MATa bar1 cln1ΔclTRP cln2Δ::LEU CLN3-6xHA:: HIS3*	This study	Fig. 9
DK4647	*MATa CLN3-6xHA::NATNT2 CLN2-13xMyc::KANMX*	This study	Fig. 6
DK4648	*MATa CLN3-6xHA::NATNT2 CLN2-13xMyc::KANMX tpk1(M147G) tpk2 (M164G) tpk3 (M165G)*	This study	Fig. 6
DK4731	*MATa bar1 LexA-ER-B112::HIS3 HPHNT1::(2x) lexA-ras2^{G19V} CLN3-6xHA::NATNT2 CLN2-13xMYC::KANMX whi5Δ::URA3*	This study	Fig. 8
DK4812	*MATa bar1 LexA-ER-B112::HIS3 HPHNT1::(2x) lexA-ras2^{G19V} CLN3-6xHA::NATNT2 CLN2-13xMYC::KANMX RAS2::URA3 (pJTD14A)*	This study	Fig. 4 and Supplementary Fig. 3a
DK4817	*MATa bar1 LexA-ER-B112::HIS3 HPHNT1::(2x) lexA-ras2^{G19V} CLN3-6xHA::NATNT2 CLN1-13xMYC::KANMX*	This study	Supplementary Fig. 2c

Diagenode). The sonicated material was centrifuged, and the supernatant was collected for immunoprecipitation.

Chromatin immunoprecipitations were performed overnight at 4°C using 500–700 μg of chromatin and a mouse monoclonal anti-HA antibody (12CA5, Gift of David Toczyski, University of California, San Francisco) bound to Protein A Dynabeads (Thermo Fisher #10001D). The beads were washed twice with lysis buffer (50-mM HEPES-KOH, pH 7.5, 140-mM NaCl, 1-mM EDTA, 1% Triton X-100, 0.1% sodium deoxycholate), twice with high salt buffer (lysis buffer with 500-mM NaCl), twice with LiCl buffer (0.5% deoxycholic acid, 1-mM EDTA, 250-mM LiCl, 0.5% NP-40, 10-mM Tris–HCl, pH 8.0), and once with TE buffer (10-mM Tris–HCl, pH 8.0, 1-mM EDTA). Cross-links were reversed overnight in elution buffer (5-mM EDTA, 0.5% SDS, 0.3-mM NaCl, 10-mM Tris–HCl, pH 8.0) at 65°C. DNA was purified using the ChIP DNA Clean & Concentrator purification kit (Zymo #D5201). Quantitative PCR reactions were performed using a detection system (LightCycler480 II; Roche). A standard curve representing a range of concentrations of input samples was used for quantifying the amount of product for each sample with each primer set. All ChIP samples were normalized to corresponding input control samples, to a genomic reference region on chromosome I, and to a genetically identical untagged strain as a control (ChIP primers for the *CLN2* promoter region: *CAATTCATGCGCGCTTTACC, TCTTCGCTAGGTATCCGCAT*. ChIP primers for the chromosome I control region: *GTTTATAGCGGGCATTATGCGTAGATCAG* and *GTTCCTCTAGAATTTTTCCACTCGCACA-TT*).

Western blotting and quantification

For western blotting, 1.6-mL samples were taken from cultures and pelleted in a microfuge at 13,200 rpm for 30 seconds before aspirating the supernatant and adding 250 μL of glass beads and freezing on liquid nitrogen. Cells were lysed in 140 μL of 1× SDS-PAGE sample buffer (65-mM Tris–HCl, pH 6.8, 3% SDS, 10% glycerol, 100-mM β-glycerophosphate 50-mM NaF, 5% β-mercaptoethanol, 2-mM PMSF, and bromophenol blue) by bead beating in a Biospec Mini-Beadbeater-16 at 4°C for 2 minutes. The lysate was centrifuged for 15 seconds to bring the sample to the bottom of the tube and was then incubated in a 100°C water bath for 5 minutes followed by a centrifugation for 5 minutes at 13,200 rpm. Lysates were loaded onto 10% acrylamide SDS-PAGE gels that were run at a constant current setting of 20 mA per gel at 165 V. Gels were transferred to nitrocellulose membrane in a BioRad Trans-Blot Turbo Transfer system. Blots were probed overnight at 4°C in 4% milk in western wash buffer (1× PBS + 250-mM NaCl + 0.1% Tween-20) with mouse monoclonal anti-HA antibody (12CA5, Gift of David Toczyski, University of California, San Francisco), mouse monoclonal anti-Myc (2276S from Cell Signaling), polyclonal anti-Clb2 antibody, polyclonal anti-Nap1 antibody, polyclonal anti-Ypk1 antibody, or polyclonal rabbit anti-T662P antibody (Gift from Ted Powers, University of California, Davis). Western blots using anti-T662P antibody were first blocked using TBST (10-mM Tris-Cl, pH 7.5, 100-mM NaCl, and 0.1% Tween-20) + 4% milk, followed by 1 wash with TBST, then overnight incubation with anti-T662P antibody in TBST + 4% BSA. Western blots were incubated in secondary donkey anti-mouse (GE Healthcare NA934V) or donkey anti-rabbit (GE Healthcare NXA931 or Jackson Immunoresearch 711-035-152) antibody conjugated to HRP at room temperature for 60–90 minutes before imaging with Advansta ECL chemiluminescence reagents in a BioRad ChemiDoc imaging system. Western blots were quantified using BioRad Imagelab software v6.0.1. Relative

signal was calculated by normalizing to a loading control and then setting all other samples to a reference of either the zero-minute time point for time-course experiments or to wild type for log-phase comparisons (see figure legends for details).

Analysis of cell size and bud emergence

Yeast cells were grown overnight at 22°C to mid-log phase (OD600 less than 0.7). Cells were fixed with 3.7% formaldehyde for 30 minutes and were then washed with PBS + 0.02% Tween-20 + 0.1% sodium azide before measuring cell size using a Z2 Coulter Counter as previously described (Lucena *et al.* 2018) using Z2 AccuComp v3.01a software. For log phase cultures, each cell size plot is an average of 3 independent biological replicates in which each biological replicate is the average of 2 technical replicates. The percentage of budded cells was calculated by counting >200 cells at each time point using a Zeiss Axioskop 2 (Carl Zeiss).

Centrifugal elutriation

Cells were grown in YPG/E medium overnight to OD_{600} 0.4–0.8 at 30°C. Cells were harvested by spinning at 4,000 rpm in a JLA 8.1 rotor at 4°C for 6 minutes. Cell pellets were resuspended in ~100-mL cold YPG/E, then sonicated for 1 minute at duty cycle 0.5 at lowest power setting with a Braun-Sonic U sonicator with a 2000U probe at 4°C. Cells were loaded onto a Beckman JE-5.0 elutriator at 2,900 rpm at 8°C. After all cells were loaded, fluid flow was continued for 10 minutes to allow equilibration. Pump speed was then increased gradually to collect small unbudded cells, which were collected and pelleted by spinning in a JA-14 rotor at 5,000 rpm for 5 minutes. Cells were resuspended into fresh YPD medium at OD_{600} 0.4–0.6 and split into 2 cultures, and 200-nM estradiol was added to one of the cultures before incubating both cultures at 30°C. For western blotting, 1.6-mL samples were collected at each time point as cells progressed through G1 phase. Since the cells do not divide during the time course, a constant number of cells are collected at each time point so that signals are intrinsically normalized on a per cell basis. Thus, western blot signals represent protein copy number per cell. For Coulter counter and budding analysis, samples were collected and fixed with 3.7% formaldehyde for 15–30 minutes. Median cell size was calculated by the Coulter AccuComp software for each time point to plot cell size during growth in G1 phase.

Experimental replicates and statistical analysis

All experiments were repeated for a minimum of 3 biological replicates. Biological replicates are defined as experiments that are carried out on different days with different cultures. Figures present data from representative biological replicates, and Coulter counter data represent the average of biological replicates. For the statistical analyses, 1-tailed unpaired *t* test was performed using Prism 9 (GraphPad. *P*-values are described in each figure legend.

Results

Hyperactive Ras increases cell size in budding yeast

Previous experiments examined the effects of hyperactive Ras expressed from the endogenous promoter on cell size in a mutant background (Baroni *et al.* 1989). We therefore started by analyzing the effects of hyperactive Ras on cell size in an otherwise wildtype background. A hyperactive version of RAS2 can be generated by mutating glycine 19 to a valine (*ras2*^{G19V}), which is analogous to oncogenic versions of mammalian Ras. We generated a strain that expresses *ras2*^{G19V} from the endogenous promoter and measured cell size with a Coulter Counter. The *ras2*^{G19V} allele caused an increase in cell size (Fig. 1a). The effects of *ras2*^{G19V} were slightly stronger in a *ras1Δ* background (Supplementary Fig. 1a).

As an independent means of generating hyperactive Ras, we deleted 1 of the GAPs that contribute to inactivation of Ras. GAPs for Ras are encoded by 2 partially redundant paralogs referred to as *IRA1* and *IRA2*. Deletion of *IRA2* causes cells to proliferate more slowly, whereas deletion of *IRA1* does not have an obvious phenotype. Deletion of both genes is lethal. We found that *ira2Δ* caused an increase in cell size, which provided further evidence that hyperactive Ras influences cell size (Fig. 1b). A previous genome-wide search for gene deletions that influence cell size also found that *ira2Δ* causes increased cell size (Jorgensen *et al.* 2002). We next tested the effects of loss of function of Ras1 and Ras2. While *ras1Δ* did not affect cell size, *ras2Δ* caused a modest decrease (Fig. 1c and Supplementary Fig. 1b). Together, these results provide additional evidence that Ras activity influences cell size.

An inducible and titratable system for expression of *ras2*^{G19V} in yeast

A previous study found that *ras2*^{G19V} causes decreased viability (Toda *et al.* 1985), and we found that *ras2*^{G19V} cells show a large reduction in the rate of proliferation and rapidly accumulate suppressor mutations. The effects of hyperactive Ras on cell size could therefore be an indirect consequence of long-term adaptation to constitutive Ras activity. To circumvent this problem, we utilized an estradiol-inducible promoter to achieve tight temporal and titratable control of *RAS* gene expression in a nutrient independent manner (Ottoz *et al.* 2014). Briefly, cells were engineered to express a fusion protein that includes the bacterial LexA DNA-binding domain, the human estrogen receptor (ER), and a transcriptional activation domain (AD). In addition, a promoter containing 2 LexA binding sites was integrated in front of the wild-type endogenous RAS2 coding sequence or in front of *ras2*^{G19V}. In this context, addition of β-estradiol drives transcription of RAS2 or *ras2*^{G19V} (Fig. 2a).

To determine the time required to reach peak protein expression, we created strains that express RAS2-3x*HA* and *ras2*^{G19V}-3x*HA* from the *lexA* promoter (*lexA*-RAS2-3x*HA* and *lexA*-*ras2*^{G19V}-3x*HA*). Peak protein expression was reached within 60–90 minutes after addition of estradiol (Fig. 2b). Moreover, we found that 200-nM estradiol induced expression of *lexA*-RAS2-3x*HA* and *lexA*-*ras2*^{G19V}-3x*HA* at protein levels similar to RAS2-3x*HA* expressed from the endogenous promoter.

For analysis of *ras2*^{G19V} phenotypes, we utilized untagged versions of RAS2 (*lexA*-RAS2 and *lexA*-*ras2*^{G19V}). We first tested the effects of inducing expression of *ras2*^{G19V} on cell proliferation. Serial dilutions of cells containing *lexA*-*ras2*^{G19V} and control cells were plated on media containing increasing concentrations of estradiol. Expression of *ras2*^{G19V} at endogenous levels (100–200-nM estradiol) caused a large reduction in the rate of proliferation (Fig. 2c). Expression at higher levels of *ras2*^{G19V} with 400-nM estradiol was nearly lethal.

We next tested whether expression of *ras2*^{G19V} from the *lexA* promoter causes an increase in cell size. Prolonged expression of *ras2*^{G19V} for 12 hours caused a large increase in cell size (Fig. 2d). The increase in cell size was detectable within 3 hours of inducing expression, which suggests that it is a rapid and direct consequence of *ras2*^{G19V} expression (Fig. 2e).

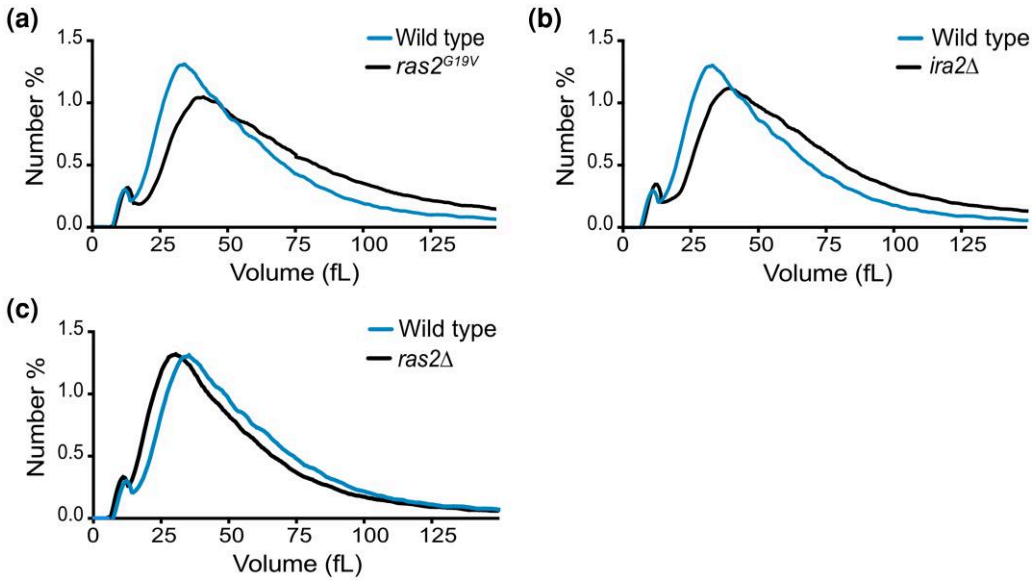

Fig. 1. Hyperactive Ras increases cell size. a) Wildtype and *ras2*^{G19V} yeast cells were grown to log phase in YPD, and cell size was measured using a Coulter counter. b) Wildtype and *ira2Δ* budding yeast cells were grown to log phase in YPD, and cell size was measured using a Coulter counter. c) Wildtype and *ras2*Δ budding yeast cells were grown to log phase in YPD, and cell size was measured using a Coulter counter.

Expression of *ras2*^{G19V} influences cell cycle progression and cell size

We next set out to learn more about how *ras2*^{G19V} influences cell size. To do this, we first analyzed how *ras2*^{G19V} influences the relationship between cell growth and cell cycle progression. Previous studies analyzed the effects of hyperactive Ras on the cell cycle indirectly by manipulating cAMP levels to mimic Ras-dependent signals that control PKA, or by deleting the BCY1 gene, which leads to a high level of constitutive PKA signaling (Matsumoto *et al.* 1983; Toda *et al.* 1987; Baroni *et al.* 1994; Tokiwa *et al.* 1994; Hall 1998; Mizunuma *et al.* 2013; Amigoni *et al.* 2015). Together, these studies suggested a link between cAMP-dependent signaling and regulation of G1 cyclin expression; however, in some cases, the studies reached conflicting conclusions. For example, 2 studies found that cAMP-dependent signaling stimulates production of *CLN3* mRNA (Tokiwa *et al.* 1994; Mizunuma *et al.* 2013) whereas other studies observed no effect (Hubler *et al.* 1993; Hall 1998). Similarly, several studies found that cAMP-dependent signaling increases transcription of *CLN1* and *CLN2* (Hubler *et al.* 1993; Hall 1998) whereas 2 other studies reported a decrease in transcription (Baroni *et al.* 1994; Tokiwa *et al.* 1994). Differences in results could be due to technical differences in how the experiments were carried out.

Previous investigations were limited by the tools available at the time and were unable to analyze the immediate effects of Ras-dependent signaling on the cell cycle. Moreover, although production of cAMP is a well-established output of Ras-dependent signaling in budding yeast, it is possible that Ras has targets beyond cAMP production. An additional limitation of previous studies is that they did not analyze how cAMP-dependent signals influence G1 cyclin protein expression during the cell cycle.

Here, we directly examined how expression of *lexA-ras2*^{G19V} influences cell cycle progression, cell growth, and cyclin expression in synchronized cells. Cells were arrested in G1 phase with mating pheromone and expression of RAS2 or *ras2*^{G19V} from the *lexA* promoter was induced prior to release from the arrest. Wildtype cells that express RAS2 from the endogenous promoter were included as a control. Since bud emergence marks cell cycle entry, we first analyzed the percentage of cells undergoing bud emergence as a function of time. Expression of *lexA-ras2*^{G19V} caused a prolonged delay in bud emergence (Fig. 3a). We also analyzed cell size as a function of time with a Coulter Channelyzer (Fig. 3b) and plotted bud emergence as a function of cell size (Fig. 3c). *ras2*^{G19V} caused cells to undergo bud emergence at a larger cell size. Previous studies found that increased levels of cAMP cause similar effects on cell size at cell cycle entry (Tokiwa *et al.* 1994; Amigoni *et al.* 2015).

Expression of *ras2*^{G19V} blocks a key step in cell cycle entry

We next analyzed the effects of *ras2*^{G19V} on expression of G1 phase cyclins. In budding yeast, a cyclin called *CLN3* is expressed in early G1 phase and accumulates gradually, leading to an increase in Cln3 protein concentration (Landry *et al.* 2012; Zapata *et al.* 2014; Lucena *et al.* 2018; Litsios *et al.* 2019, 2022; Sommer *et al.* 2021). The extent of Cln3 protein accumulation in G1 phase is correlated with growth and appears to be dependent upon cell growth, which suggests that it could be a readout of the extent of growth (Sommer *et al.* 2021). Cln3 eventually triggers transcription of a redundant pair of late G1 phase cyclin paralogs called *CLN1* and *CLN2* (Tyers *et al.* 1993; Dirick *et al.* 1995; Stuart and Wittenberg 1995). Expression of late G1 phase cyclins is the key molecular event that drives cell cycle entry. To assay accumulation of both early and late G1 phase cyclins, we used a strain that contains Cln3-6xHA and Cln2-13xMyc. Wildtype, *lexA-RAS2*, and *lexA-ras2*^{G19V} cells were synchronized in G1 phase with mating pheromone, and the behavior of Cln3-6xHA and Cln2-13xMyc was assayed by western blot during the cell cycle. *ras2*^{G19V} caused a nearly 3-fold increase in the expression of Cln3-6xHA protein in G1 phase, as well as delayed and decreased expression of Cln2-13xMyc (Fig. 3d–e and Supplementary Fig. 2a). Expression of *lexA-ras2*^{G19V} also caused a decrease in Cln2-13Myc levels in asynchronously growing cells (Supplementary Fig. 2b). Previous studies analyzed how activation of PKA influences the function and regulation of Cln1, a redundant paralog of Cln2 (Baroni *et al.* 1994; Tokiwa *et al.* 1994; Hall 1998; Amigoni *et al.* 2015). These

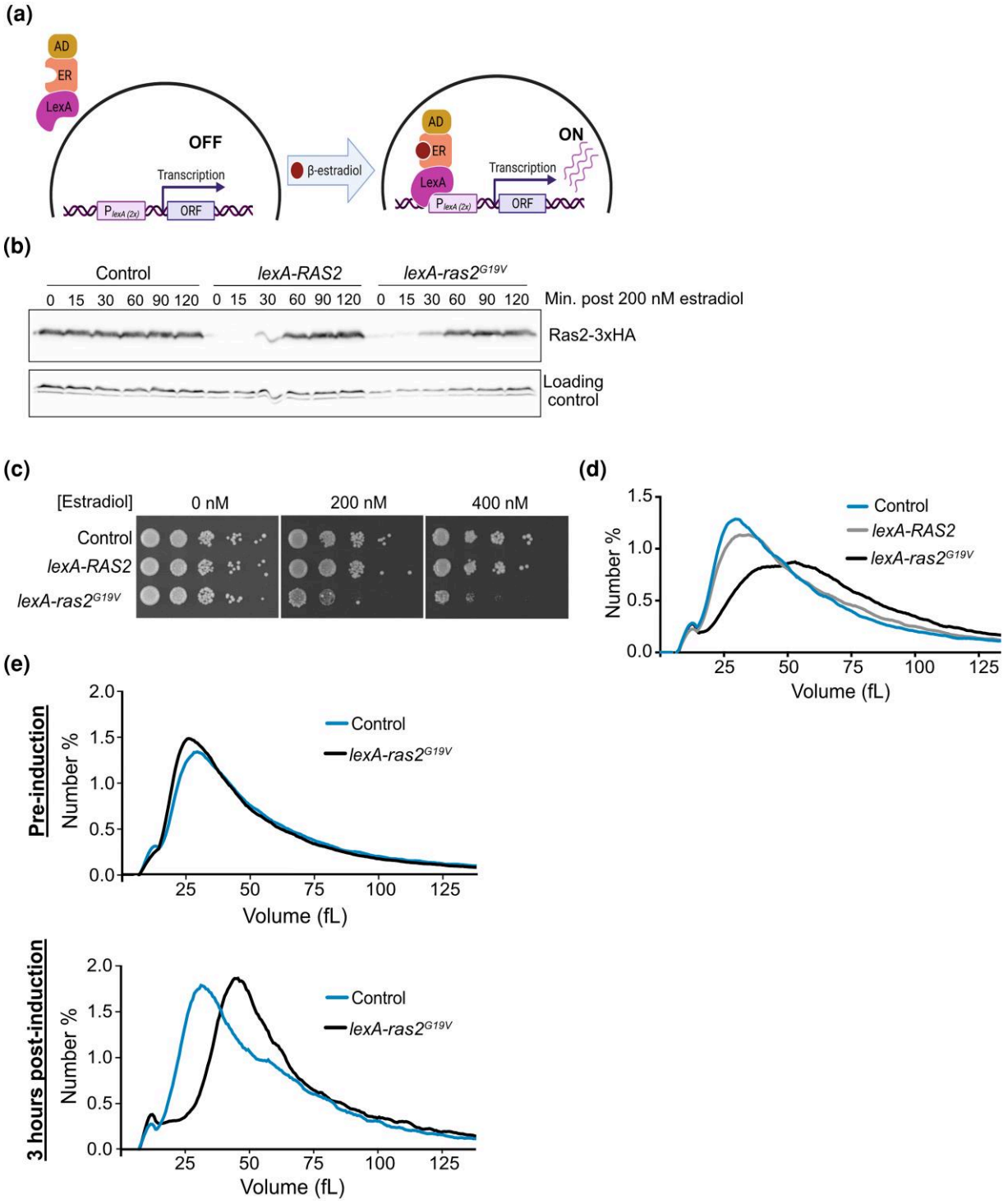

Fig. 2. An inducible and titratable expression system for expression of *ras2*^{G19V} in yeast. a) A diagram of the LexA-ER-AD system for estradiol-dependent gene expression. b) Estradiol was added to 200 nM, and time points were collected at the indicated intervals to measure timing for peak levels of Ras2 or ras2^{G19V} protein expression relative to endogenous levels. c) Serial dilutions of the indicated strains were spotted onto YPD medium containing the indicated concentrations of estradiol. d) Cells were grown overnight to log phase in YPD + 100-nM estradiol, and cell size was measured using a Coulter counter. e) Cells were grown overnight to log phase in YPD and expression of *ras2*^{G19V} was induced with 100-nM estradiol for 3 hours. Cell size was measured using a Coulter Counter.

studies suggested that there may be differences in the regulation of Cln1 and Cln2. Therefore, we next tested how expression of *lexA-ras2*^{G19V} influences expression of Cln1. We found that expression of *lexA-ras2*^{G19V} caused delayed and decreased expression of Cln1-13xMyc, similar to Cln2-13xMyc (Supplementary Fig. 2c).

To further test the effects of expressing *ras2*^{G19V}, we used centrifugal elutriation as an independent means of synchronizing cells in G1 phase. For this approach, cells are first grown in poor carbon medium, which generates a large population of very small newborn cells in G1 phase. After isolation of newborn cells, they

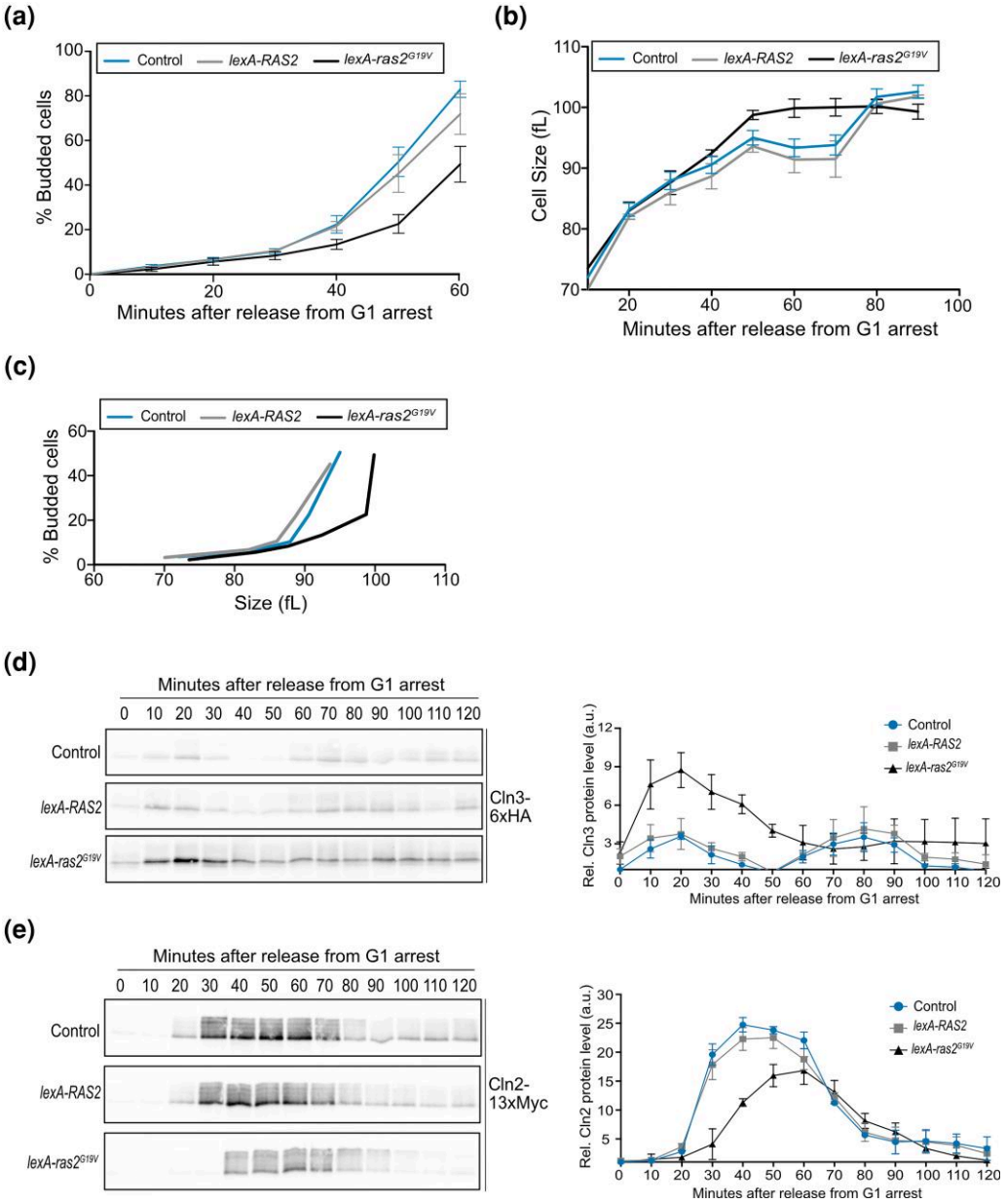

Fig. 3. Expression of *ras2*^{G19V} influences cell size, delays cell cycle entry, and influences expression of G1 phase cyclins in synchronized cells. a–c) Cells were grown to log-phase overnight in YPD and were then arrested in G1 phase with alpha factor for 3 hours at 30°C. Cells were treated with 200-nM estradiol beginning 1.5 hours before release from the arrest. a) The percentage of budded cells as a function of time. b) Median cell size was measured at 10-minute intervals using a Coulter Counter and plotted as a function of time. c) The percentage of budded cells as a function of cell size. Error bars represent SEM of 3 biological replicates. d–e) Cells were grown to log-phase overnight in YPD and were then arrested in G1 phase with alpha factor for 3 hours at 30°C. Expression of RAS2 or *ras2*^{G19V} was induced with 200-nM estradiol beginning 1.5 hours before release from the arrest. d) The levels of Cln3-6xHA protein were analyzed by western blot. e) The levels of Cln2-13xMyc protein were analyzed by western blot. The representative western blots in d) and e) are from the same experiment, and protein abundance was quantified relative to levels in wildtype cells at time point 0 after first normalizing to a loading control (loading controls are shown in Fig. 3–Supplementary Fig. 1a). Error bars represent SEM of 3 biological replicates. For both plots, protein abundance was plotted as a ratio over the signal in wildtype control cells at $t = 0$ after first normalizing to the loading control.

are shifted to rich carbon medium, where they undergo a prolonged interval of growth in G1 phase to reach the higher threshold of growth required for cell cycle entry in rich carbon. Cells in which the endogenous RAS2 promoter has been replaced by the lexA promoter do not proliferate in poor carbon medium because RAS2 is required for growth in poor carbon sources (Tatchell *et al.* 1985). Therefore, we generated a new *lexA-ras2*^{G19V} strain that also carries a wildtype copy of the RAS2 gene integrated at URA3. We isolated newborn *lexA-ras2*^{G19V} cells and released them into YPD medium with or without estradiol. Expression of Cln3-6XHA and Cln2-13Myc was assayed by western blot. We also assayed bud emergence and median cell size at regular intervals. Expression of *ras2*^{G19V} again caused a large increase in Cln3 protein levels, delayed bud emergence, and reduced expression of Cln2 (Fig. 4a–e and Supplementary Fig. 3). Expression of *ras2*^{G19V} did not influence growth rate (Fig. 4b).

Previous studies suggested that increased expression of *CLN3* drives premature cell cycle entry (Cross 1988; Nash *et al.* 1988;

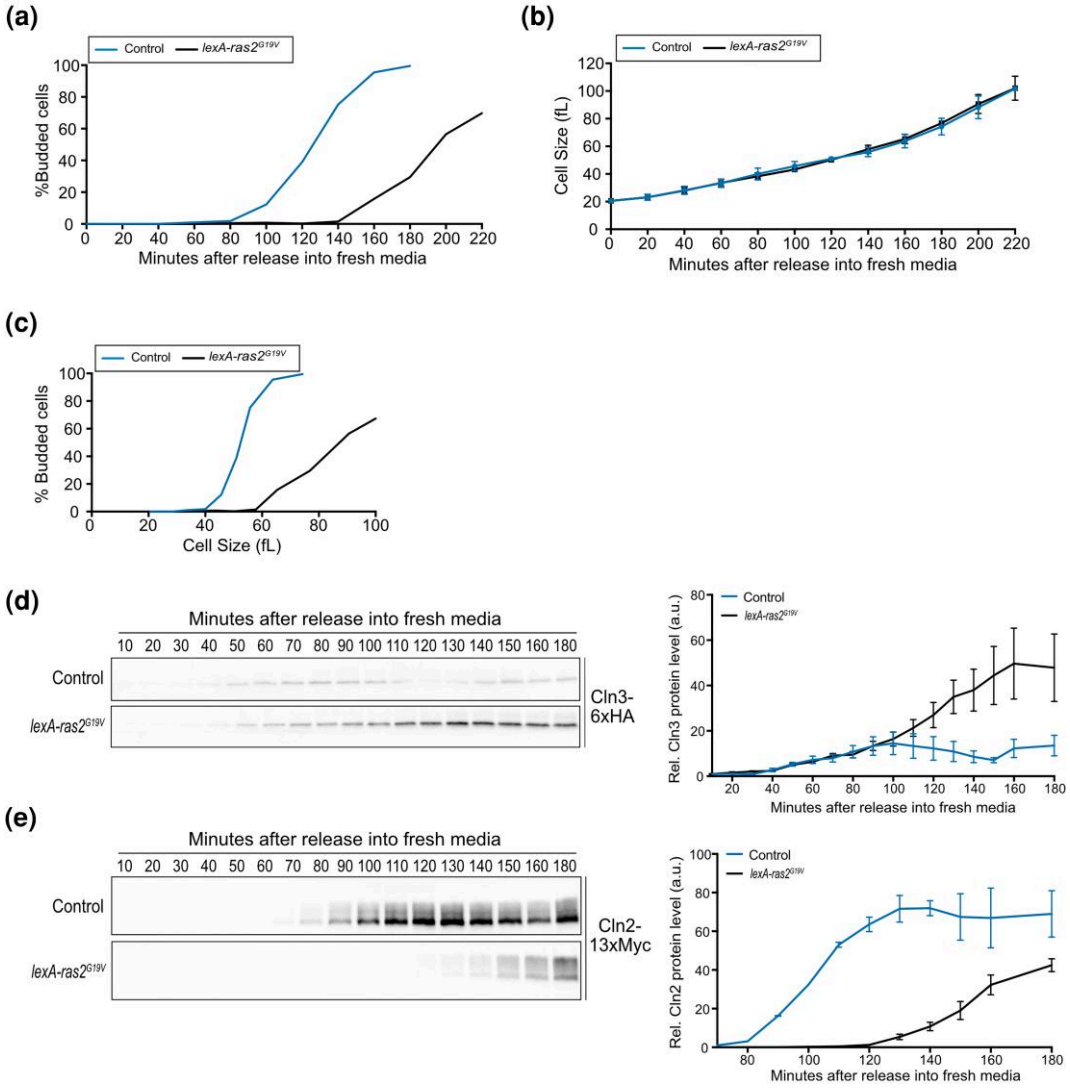

Fig. 4. Expression of *ras2*^{G19V} influences cell size, delays cell cycle entry, and influences expression of G1 phase cyclins in cells synchronized by centrifugal elutriation. a–c) Cells were grown to mid-log phase in poor carbon (YPG/E), and small unbudded cells were isolated by centrifugal elutriation. Cells were released into YPD media at 30°C, and samples were collected at the indicated intervals. a) The percentage of budded cells as a function of time. b) Median cell size was measured using a Coulter Counter at 20-minute intervals and plotted as a function of time. c) The percentage of budded cells as a function of median cell size at each time point. d) The levels of Cln3-6xHA protein were analyzed by western blot. e) The levels of Cln2-13xMyc protein were analyzed by western blot. The western blots in a) and b) are from the same experiment, and protein abundance was quantified relative to levels in wildtype cells at time point 0 after first normalizing to a loading control (loading controls are shown in Fig. 4–Supplementary Fig. 1). Error bars represent SEM of 3 biological replicates.

Nasmyth and Dirick 1991). Thus, the finding that *ras2*^{G19V} strongly promotes expression of Cln3, yet inhibits expression of Cln2, was unexpected.

We next used northern blotting to test whether *ras2*^{G19V} influences transcription of *CLN2*. *ras2*^{G19V} caused a delay in *CLN2* transcription and a reduction of *CLN2* mRNA levels (Fig. 5a). To test whether *ras2*^{G19V} also influences expression of *CLN2* via post-transcriptional mechanisms, we replaced the endogenous *CLN2* promoter with the heterologous *MET25* promoter. The *MET25* promoter drives a basal level of constitutive expression in medium that contains methione. A higher level of transcription can be induced by withdrawal of methionine. Here, we used basal uninduced transcription from the *MET25* promoter to express *CLN2*. In this context, *ras2*^{G19V} no longer delayed Cln2 protein expression and caused a small decrease in protein levels, although it was unclear whether the decrease was significant (Fig. 5b). These data show that *ras2*^{G19V} influences *CLN2* expression largely via transcriptional mechanisms that are dependent upon features of the *CLN2* promoter.

Induction of late G1 cyclin transcription by Cln3 is thought to be the critical molecular step that initiates cell cycle entry. It is also thought to be the step where cell growth influences cell cycle entry. Thus, the discovery that expression of *ras2*^{G19V} promotes high level expression of Cln3, yet fails to induce normal expression of Cln2, suggests that *ras2*^{G19V} inhibits a key step in cell cycle entry.

ras2^{G19V} causes decreased recruitment of Cln3 to the *CLN2* promoter

Previous work has shown that Cln3 is recruited to promoters controlled by SBF, including the *CLN2* promoter, where it has been proposed to activate Cdk1 to directly phosphorylate RNA polymerase (Wang *et al.* 2009; Kõivomägi *et al.* 2021). To test whether

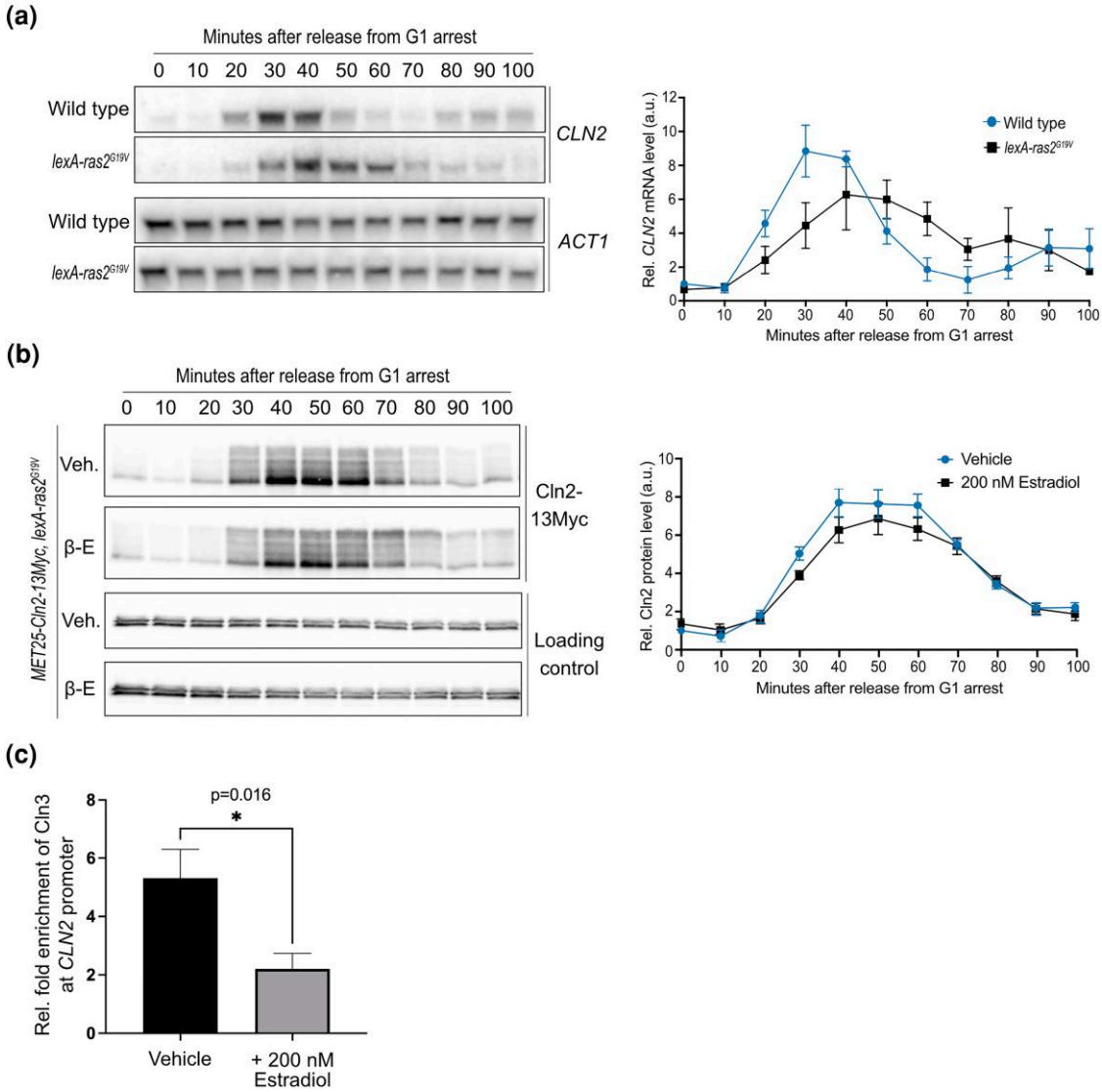

Fig. 5. Expression of *ras2*^{G19V} modulates Cln2 protein expression at the level of transcription. a–b) Cells were grown to log-phase overnight in YPD and were then arrested in G1 phase with alpha factor for 3 hours at 30°C. Expression of *RAS2* or *ras2*^{G19V} was induced with 200-nM estradiol beginning 1.5 hours before release from the arrest. a) Levels of *CLN2* mRNA were analyzed by northern blot. Levels of the *ACT1* mRNA were analyzed as a loading control. After normalizing to the loading control, the *CLN2* mRNA signal was quantified and plotted as a ratio over the signal at $t = 0$ in the wild control cells. Error bars represent SEM of 3 biological replicates. b) Levels of Cln2-13xMyc protein were analyzed by western blot. Protein abundance was plotted as a ratio over the signal in wildtype cells at $t = 0$ after first normalizing to the loading control. Error bars represent SEM of 3 biological replicates. An anti-Nap1 antibody was used for a loading control. c) For ChIP experiments, cells were grown to log-phase overnight in YPD and expression of *RAS2* or *ras2*^{G19V} was induced with 200-nM estradiol for 3 hours at 30°C. Cln3-6xHA was immunoprecipitated, and qPCR was conducted to determine relative fold enrichment of Cln3-6xHA at the *CLN2* promoter. *$P = 0.016$ by Student's *t* test.

ras2^{G19V} disrupts recruitment of Cln3 to the *CLN2* promoter, we used ChIP to analyze recruitment of Cln3 to *CLN2* promoters in *lexA-ras2*^{G19V} cells. We found that *ras2*^{G19V} caused a 3-fold reduction in the amount of Cln3 that is recruited to the *CLN2* promoter (Fig. 5c). The mechanisms by which Cln3 is recruited to the *CLN2* promoter are unknown so we are unable to define the molecular defect that obstructs Cln3 recruitment.

PKA influences cell size and expression of G1 phase cyclins

The fact that Ras activates PKA suggests that the effects of *ras2*^{G19V} on cell size could be mediated by PKA. Furthermore, it has been proposed that PKA can influence expression of G1 phase cyclins via inhibition of Whi3, an RNA-binding protein that is thought to bind and inhibit the expression of dozens of mRNAs, including those for *CLN2* and *CLN3* (Wang *et al.* 2004; Cai and Futcher 2013; Mizunuma *et al.* 2013). *WHI3* was originally discovered in a screen for loss of function mutants that cause reduced cell size (Nash *et al.* 2001). Although 1 study found no effect of *whi3Δ* on Cln3 protein expression (Garí *et al.* 2001), a more recent study found that *whi3Δ* causes an increase in the abundance and translation efficiency of the *CLN3* mRNA, which could account for the reduced cell size of *whi3Δ* cells (Wang *et al.* 2004; Cai and Futcher 2013). Mutation of a PKA consensus site within Whi3 causes reduced binding of Whi3 to *CLN3* mRNA; however, it remains unknown whether this site is phosphorylated by PKA in vivo (Mizunuma *et al.* 2013). Together, these observations suggest a model in which *ras2*^{G19V} influences G1 phase cyclin levels and cell size via PKA-dependent inhibition of Whi3.

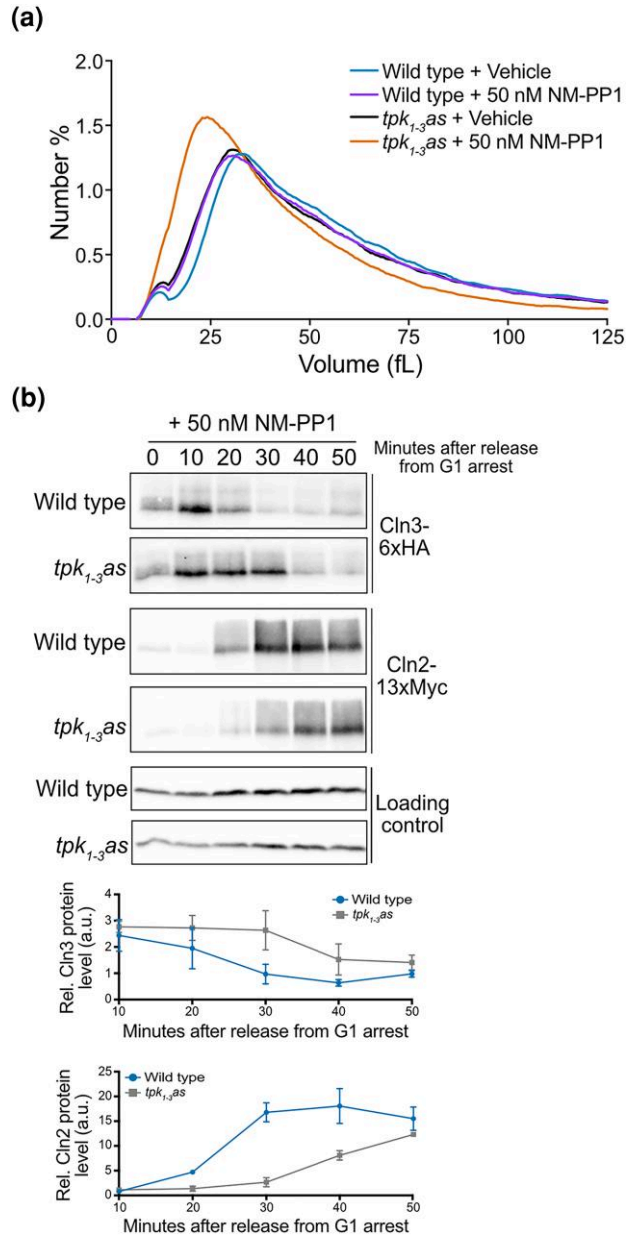

Fig. 6. PKA activity influences cell size and expression of G1 phase cyclins. a) Cells were grown overnight to log phase in YPD + vehicle or 50-nM 1NM-PP1, and cell size was measured using a Coulter Counter. b) Cells were grown to log-phase overnight in YPD and were then arrested in G1 phase with alpha factor for 3 hours at 30°C. Cells were released from the arrest into YPD containing 100-nM 1NM-PP1. The levels of Cln3-6xHA and Cln2-13xMyc protein were analyzed by western blot. Protein abundance was plotted as a ratio over the signal in wildtype cells at $t = 0$ after first normalizing to the loading control. Error bars represent SEM of 3 biological replicates. Anti-Nap1 was used for a loading control.

To begin to test this model, we first analyzed the effects of modulating PKA activity on cell size and cell cycle progression. Previous studies tested the effects of increased PKA activity by deleting the *BCY1* gene, which encodes the inhibitory subunit for PKA (Matsumoto *et al.* 1983; Toda *et al.* 1985, 1987; Guerra *et al.* 2022). Loss of *BCY1* leads to increased cell size (Baroni *et al.* 1994; Tokiwa *et al.* 1994). However, we found that *bcy1Δ* is lethal in the strain background used here (W303) and that a C-terminal auxin-inducible degron tag causes loss of function of Bcy1. We therefore used an analog-sensitive version of PKA to analyze the effects of decreased PKA activity. PKA in budding yeast is encoded by 3 redundant genes referred to as *TPK1*, *TPK2*, and *TPK3*. A previous study generated a strain in which all 3 *TPK* genes carry mutations that make them sensitive to the adenine analog inhibitor 1NM-PP1 (*pka-as*) (Zaman *et al.* 2009). If the effects of $ras2^{G19V}$ are due to hyperactive PKA, then reduced activity of PKA would be expected to cause effects that are opposite to the effects of hyperactive Ras alone.

We found that *pka-as* cells showed substantially reduced cell size in response to a nonlethal dose of inhibitor (50 nM) (Fig. 6a). Inhibition of PKA at this level had little effect on peak levels of Cln3, although it did prolong the interval of expression of Cln3 in G1 phase (Fig. 6b). Expression of Cln2 protein was reduced and delayed, similar to the effects of $ras2^{G19V}$.

The observed effects of inhibiting PKA are difficult to reconcile with simple models for $ras2^{G19V}$ functions based on previous studies. The discovery that $ras2^{G19V}$ and inhibition of PKA have opposite effects on cell size would appear to be consistent with a model in which $ras2^{G19V}$ drives an increase in cell size via hyperactivation of PKA. However, the discovery that $ras2^{G19V}$ and inhibition of PKA have similar effects on Cln2 protein levels suggests that the effects caused by hyperactive Ras cannot be explained solely by changes in the activity of PKA. Rather, the data suggest that hyperactive Ras signaling could be influencing Cln2 levels via PKA-independent mechanisms.

The effects of $ras2^{G19V}$ are not due solely to inhibition of Whi3

To investigate the relationship between $ras2^{G19V}$ signaling and Whi3, we compared cell size, timing of bud emergence, and expression of Cln3 and Cln2 protein in wildtype, *whi3Δ*, *lexA-*$ras2^{G19V}$, and *lexA-*$ras2^{G19V}$ *whi3Δ* cells. If $ras2^{G19V}$ influences expression of Cln3 or Cln2 via PKA-dependent inhibition of Whi3, one would expect *whi3*Δ and $ras2^{G19V}$ to cause similar effects on expression of Cln3 and Cln2 protein levels.

We found that *whi3*Δ accelerated the timing of bud emergence and caused reduced cell size, as expected (Fig. 7a and b). Moreover, in contrast to a previous study (Garí *et al.* 2001), we found that *whi3Δ* caused a substantial increase in Cln3 protein levels (Fig. 7c and Supplementary Fig. 4a). *whi3Δ* also caused a strong increase in the second peak of Cln3 later in the cell cycle. Note that alpha factor was added back to the cells to prevent a second cell cycle, so the second peak in Cln3 levels corresponds to the second mitotic peak of Cln3 that has been reported previously (Landry *et al.* 2012; Zapata *et al.* 2014). *whi3Δ* also accelerated expression of Cln2 protein, as expected for increased Cln3 protein levels (Fig. 7d and Supplementary Fig. 4a).

The effects of *lexA-*$ras2^{G19V}$ expression and *whi3Δ* on Cln3 protein levels were similar, as both caused a substantial increase in Cln3 protein levels. Moreover, the effects of *whi3Δ* and *lexA-*$ras2^{G19V}$ on peak Cln3 protein levels were not additive in G1 phase in *lexA-*$ras2^{G19V}$ *whi3Δ* cells. Thus, it is possible that $ras2^{G19V}$ drives an increase in Cln3 protein levels via PKA-dependent inhibition of Whi3, as suggested by a previous study that found evidence for PKA-dependent inhibition of Whi3 (Mizunuma *et al.* 2013). However, *whi3Δ* and expression of *lexA-*$ras2^{G19V}$ caused opposite effects on the timing of bud emergence, cell size, and accumulation of Cln2 protein. Thus, the effects of $ras2^{G19V}$ cannot be explained solely by inhibition of Whi3.

The effects of $ras2^{G19V}$ on late G1 phase cyclin expression are dependent upon Whi5

Genetic data suggest that Cln3 promotes transcription of *CLN2* at least partly via inhibition of Whi5, which binds and inhibits the SBF transcription factor that promotes *CLN2* transcription (Costanzo *et al.*

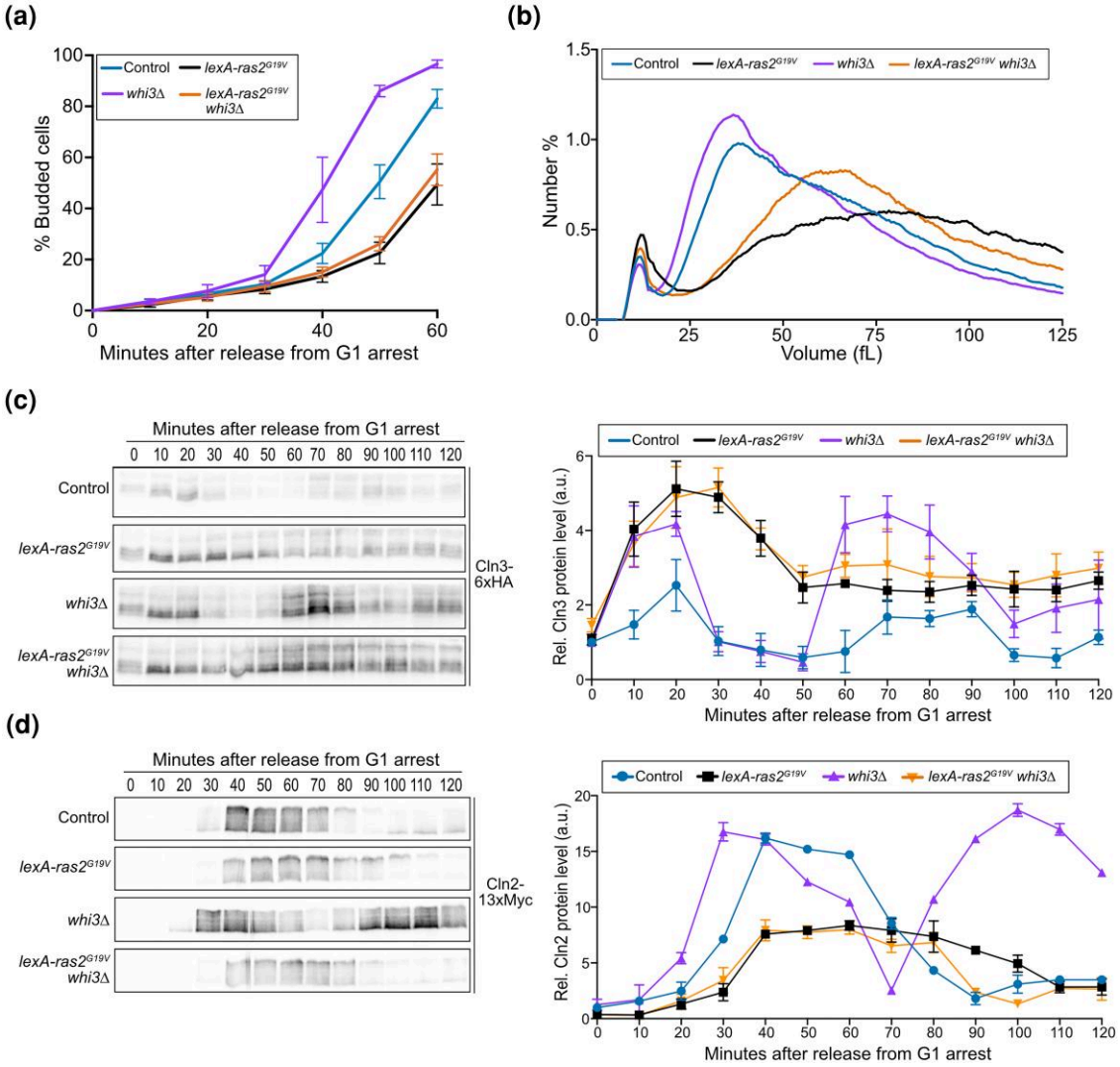

Fig. 7. The effects of *ras2*^{G19V} are not due solely to inhibition of Whi3. a–c) Cells were grown to log-phase overnight in YPD and were then arrested in G1 phase with alpha factor for 3 hours at 30°C. Cells were treated with 200-nM estradiol beginning 1.5 hours prior to release. a) The percentage of budded cells as a function of time. b) The levels of Cln3-6xHA protein were analyzed by western blot, and protein abundance was quantified relative to levels of Cln3-6xHA in wildtype cells at t = 0 after first normalizing to a loading control. The loading control is shown in Fig. 7–Supplementary Fig 1. Error bars represent SEM of 3 biological replicates. c) The levels of Cln2-13xMyc protein were analyzed by western blot, and protein abundance was quantified relative to levels of Cln2-13xMyc in wildtype cells at t = 0 after first normalizing to a loading control. The loading controls are shown in Fig. 7–Supplementary Fig. 1. Error bars represent SEM of 3 biological replicates. Error bars represent SEM of 3 biological replicates. d) Cells were grown overnight to log phase in YPD + 100-nM estradiol, and cell size was measured using a Coulter counter.

2004; de Bruin *et al.* 2004). We found that *whi5Δ* largely rescued the delays in Cln2 expression and cell cycle progression caused by *ras2*^{G19V} (Fig. 8a). This observation provides further support for the idea that expression of *lexA-ras2*^{G19V} blocks a key step in the mechanisms by which Cln3 initiates transcription of *CLN2*, and it suggests that *ras2*^{G19V} may prevent inhibition of Whi5. However, the mechanisms by which Cln3 promotes inhibition of Whi5 are poorly understood (Bhaduri *et al.* 2015; Kõivomägi *et al.* 2021).

Deletion of *WHI5* only partially rescued the cell size defects caused by *ras2*^{G19V}, which suggests that *ras2*^{G19V} influences cell size via mechanisms that operate outside of G1 phase (Fig. 8b). Consistent with this possibility, previous studies have found evidence that Ras influences mitotic exit (Morishita *et al.* 1995; Seshan and Amon 2005).

Cln2 may influence expression of Cln3 via negative feedback

ras2^{G19V} and inhibition of PKA both caused Cln3 protein to persist for a longer interval in G1 phase (Figs. 4a, 6b, and 7c). In each context, prolonged expression of Cln3 protein was accompanied by reduced and delayed accumulation of Cln2. A potential explanation for these observations is that Cln2 is required for downregulation of Cln3. This kind of negative feedback regulation has been observed at other stages in the cell cycle. For example, mitotic cyclins repress expression of cyclins that appear earlier in the cell cycle (Amon *et al.* 1993). To test this idea, we determined whether gain-of or loss-of-function of *CLN1/2* influences expression of Cln3 protein in synchronized cells. We found that over-expression of *CLN2* from the *GAL1* promoter led to substantially lower levels of Cln3 protein during G1 phase, as well as a premature reduction in Cln3 protein levels (Fig. 9a). Conversely, loss of function of Cln1/2 in *cln1Δ cln2Δ* cells appeared to cause increased Cln3 protein expression during G1 phase (Fig. 9b). A caveat is that the *cln1Δ cln2Δ* cells did not fully synchronize. Therefore, we also analyzed Cln3 levels in unsynchronized cells, which again appeared to show that loss of *CLN1/2* causes an increase in Cln3 protein levels (Fig. 9c).

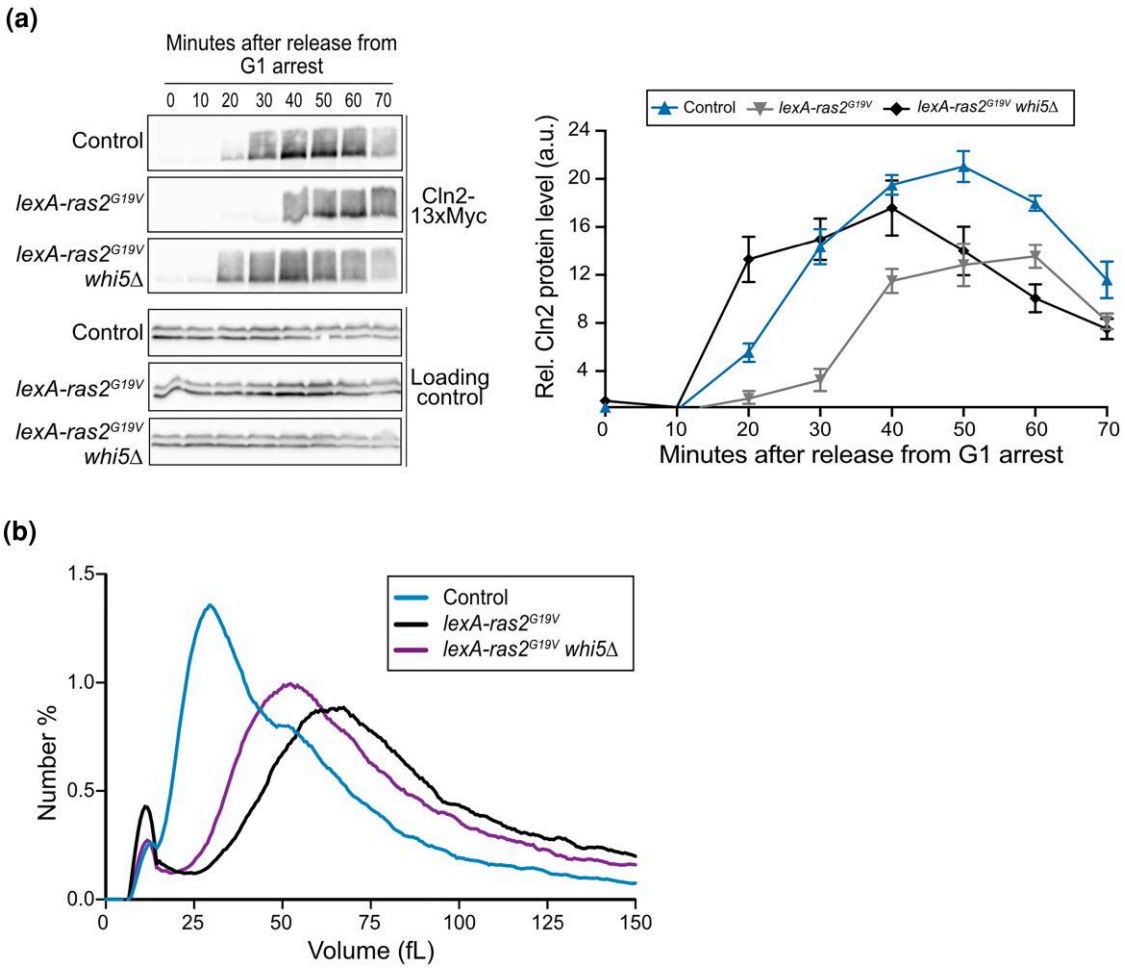

Fig. 8. The effects of *ras2*^{G19V} on late G1 phase cyclin expression are dependent upon Whi5. a) Cells were grown to log-phase overnight in YPD and then arrested in G1 phase with alpha factor for 3 hours at 30°C. Cells were treated with 200-nM estradiol beginning 1.5 hours prior to release. The levels of Cln2-13xMyc protein were analyzed by western blot, and protein abundance was quantified relative to levels of Cln2-13xMyc in wildtype cells at $t = 0$ after first normalizing to the loading control. Error bars represent SEM of 3 biological replicates. An anti-Nap1 antibody was used for a loading control. b) Cells were grown overnight to log phase in YPD + vehicle or 100-nM estradiol, and cell size was measured using a Coulter counter.

Discussion

Hyperactive Ras influences cell size and disrupts a critical step in cell cycle entry

Pioneering work carried out over 20 years ago suggested that Ras influences cell size in yeast. However, technical limitations made it difficult to determine whether size defects caused by Ras mutants were an immediate and direct consequence of aberrant Ras activity. Here, we used new methods to express Ras from an inducible promoter at endogenous levels, which provides a powerful new system in which to analyze the effects of hyperactive Ras. This allowed us to clearly establish that cell size defects are an immediate and direct consequence of *ras2*^{G19V} activity.

Several previous studies suggested that hyperactive Ras influences cell cycle progression and expression of G1 phase cyclins, which could help explain the size defects of *ras2*^{G19V} cells. However, these studies examined the effects of hyperactive Ras indirectly by manipulating PKA signaling, and in some cases obtained conflicting results (Matsumoto *et al.* 1983; Toda *et al.* 1985, 1987; Baroni *et al.* 1994; Tokiwa *et al.* 1994; Hall 1998; Mizunuma *et al.* 2013). Here, we directly tested the immediate effects of *ras2*^{G19V} expressed from an inducible promoter, which showed that *ras2*^{G19V} causes a prolonged delay before bud emergence. Growth continues during the delay so that *ras2*^{G19V} cells initiate bud emergence at a substantially larger size than control cells.

To better understand the cause of the G1 phase delay, we assayed expression of early and late G1 phase cyclins and found that *ras2*^{G19V} causes a 3-fold increase in Cln3 protein levels and also prolongs Cln3 expression in G1 phase. Increased Cln3 expression would be expected to accelerate and increase expression of Cln2. However, we found that *ras2*^{G19V} causes delayed and decreased expression of *CLN2* mRNA and protein. The effects of *ras2*^{G19V} on Cln2 protein expression appeared to occur primarily at the level of transcription, since replacing the normal promoter of *CLN2* with a heterologous promoter eliminated much of the effect of *ras2*^{G19V} on Cln2 protein expression. Thus, the data suggest that ras2^{G19V} disrupts the mechanisms by which Cln3 induces transcription of late G1 phase cyclins, which is a critical step in the molecular mechanisms that initiate entry into the cell cycle.

ras2^{G19V} is unlikely to control G1 phase cyclin expression via a simple PKA–Whi3 signaling axis

Previous studies suggested that *ras2*^{G19V} could influence G1 phase cyclin expression and cell cycle entry via a signaling axis in which Ras activates PKA to inhibit Whi3, which is thought to bind and

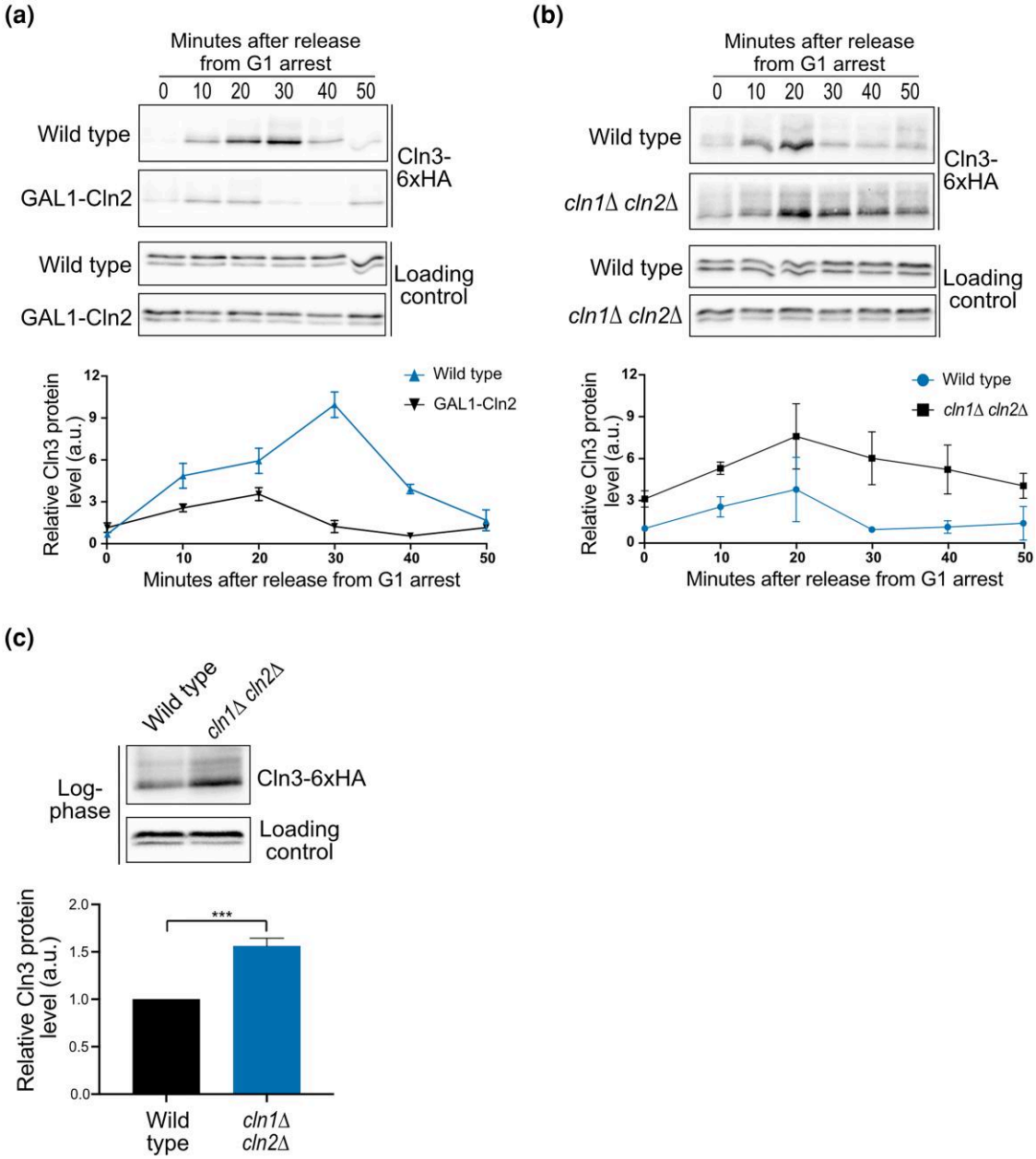

Fig. 9. Cln2 imposes negative feedback upon Cln3. a) Cells were grown to log-phase overnight in YPG/E and were then arrested in G1 phase with alpha factor for 3 hours at 30°C. Expression of GAL1-CLN2 was induced 40 minutes before release by addition of 2% galactose. Cells were washed and released into YEP containing 2% galactose. The levels of Cln3-6xHA protein were analyzed by western blot, and protein abundance was quantified relative to Cln3-6xHA levels in wildtype cells at $t = 0$ after first normalizing to the loading control. b) Cells were grown to log-phase overnight in YPD and were then arrested in G1 phase with alpha factor for 3 hours at 30°C. The levels of Cln3-6xHA protein were analyzed by western blot, and protein abundance was quantified relative to Cln3-6xHA levels in wildtype cells at $t = 0$ after first normalizing to the loading control. c) Cells were grown to log-phase overnight in YPD. Levels of Cln3-6xHA protein were analyzed by western blot, and protein abundance was quantified relative to Cln3-6xHA levels in wildtype. a–c) Error bars represent SEM of 3 biological replicates. ***$P < 0.001$ by Student's t test.

inhibit expression of G1 phase cyclin mRNAs (Garí *et al.* 2001; Cai and Futcher 2013; Mizunuma *et al.* 2013). We tested this model by comparing the effects of $ras2^{G19V}$ to the effects of *whi3Δ* or inhibition of PKA. Expression of $ras2^{G19V}$ and *whi3Δ* both caused an increase in Cln3 protein levels and a *lexA-*$ras2^{G19V}$ *whi3*Δ double mutant did not show additive effects on Cln3 protein levels. These observations are consistent with a model in which $ras2^{G19V}$ drives an increase in Cln3 protein levels via inhibition of Whi3, but do not rule out alternative models. However, the data do not support the idea that $ras2^{G19V}$ influences Cln2 protein levels via a PKA–Whi3 signaling axis. For example, $ras2^{G19V}$ and inhibition of PKA caused similar effects on Cln2 protein levels, which would not be expected if $ras2^{G19V}$ drives a decrease in Cln2 protein levels via hyperactivation of PKA. Overall, the data are most consistent with a model in which hyperactive signaling from $ras2^{G19V}$ influences Cln2 protein levels via a PKA-independent pathway. Testing this model will require additional work to define the signaling steps by which $ras2^{G19V}$ blocks normal expression of Cln2.

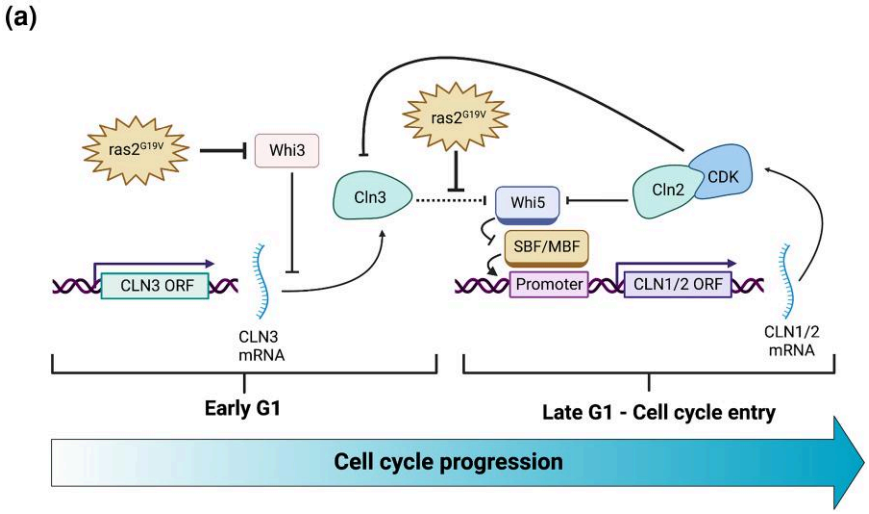

Fig. 10. Proposed model. A simplified model of the steps that control cell cycle entry in which events that appear to be influenced by *ras2*^{G19V} are highlighted.

The effects of *ras2*^{G19V} on late G1 cyclin expression are dependent upon Whi5

Previous studies suggested that Cln3 initiates transcription of late G1 phase cyclins at least partly via inhibition of Whi5 (Costanzo *et al.* 2004; de Bruin *et al.* 2004). Here, we found that expression of *ras2*^{G19V} does not delay expression of Cln2 in *whi5Δ* cells, which suggests that *ras2*^{G19V} may disrupt the mechanism by which Cln3 inactivates Whi5. Previous studies suggested that a Cln3/Cdk1 complex directly phosphorylates and inactivates Whi5; however, more recent work has definitively shown that Cln3 is not required for phosphorylation of Whi5 during cell cycle entry (Bhaduri *et al.* 2015; Kõivomägi *et al.* 2021). Thus, the mechanisms that inactivate Whi5 are poorly understood.

Whi5 appears to be functionally similar to Rb in mammalian cells, as both are repressors of late G1 phase cyclin transcription. However, Whi5 and Rb show no sequence homology and recent evidence suggests that they may be regulated via different mechanisms (Bhaduri *et al.* 2015; Kõivomägi *et al.* 2021). It has therefore remained unclear whether the mechanisms that control Whi5 and Rb are conserved. Further investigation of the mechanisms by which *ras2*^{G19V} influences Whi5 activity could therefore lead to a better understanding of the relationship between signals that control Whi5 and Rb.

The fact that deletion of *WHI5* fails to fully rescue the size defects caused by *ras2*^{G19V} suggests that constitutive Ras signaling may cause cell cycle defects outside of G1 phase. Consistent with this, previous studies have found evidence that Ras signaling regulates components of the mitotic exit network (MEN) in budding yeast (Morishita *et al.* 1995; Seshan and Amon 2005). There is also evidence that aberrant Ras signaling can lead to mitotic defects and prolonged mitotic delays in mammalian cells (Zamora-Domínguez *et al.* 2023). Therefore, it is possible that deletion of *WHI5* partially rescues the cell size defects caused by expression of *ras2*^{G19V} by rescuing the cell cycle defects in G1 phase, but fails to rescue cell cycle perturbations outside of G1 phase.

Evidence for Cln2-dependent negative regulation of Cln3

Expression of Cln2 protein was reduced and delayed by *ras2*^{G19V} and also by inhibition of PKA. In both contexts, the window of Cln3 protein expression was prolonged, which could be explained by a model in which Cln2 represses expression of Cln3. Consistent with this, we found that overexpression of Cln2 causes reduced expression of Cln3 protein, while loss of Cln1/2 appeared to increase and prolong expression of Cln3. Previous studies have shown that this kind of feedback regulation works at other times during the cell cycle in yeast (Amon *et al.* 1993). The discovery that Cln3 appears to be regulated by Cln2-dependent negative feedback suggests a new entry point for further exploration of the mechanisms that control cell cycle entry.

Analysis of aberrant Ras signaling in yeast may provide new insight into cancer cell biology

Figure 10 shows a simplified model of the mechanisms that are thought to control cell cycle entry, in which steps that appear to be influenced by *ras2*^{G19V} are highlighted (Fig. 10). Our discovery that *ras2*^{G19V} influences key steps in cell cycle entry, potentially via PKA-independent mechanisms, provides new insight into how *ras2*^{G19V} influences cell size and cell cycle progression. In mammalian cells, there is evidence that hyperactive Ras influences expression of cyclin D via mechanisms that are independent of the canonical MAP kinase signaling pathway that has been thought to mediate many functions of Ras (Kerkhoff and Rapp 1998; Muise-Helmericks *et al.* 1998; Pruitt *et al.* 2000; Pruitt and Der 2001; Coleman *et al.* 2004). In addition, human lung adenocarcinoma tumors that have oncogenic mutations in KRAS show severe cell size defects (Sandlin *et al.* 2022). Together, these observations indicate that much remains to be learned about how aberrant Ras signaling influences basic cell biology and the control of cell size. Further investigation of the mechanisms by which hyperactive Ras influences cell size and the cell cycle in yeast could yield broadly relevant insights into basic cell biology as well as cancer cell biology.

Data availability

All strains and reagents are available upon request. The authors affirm that all data necessary for confirming the conclusions of the article are present within the article, figures, and tables.

Supplemental material available at GENETICS online.

Funding

We thank Namrita Dhillon for help with chromatin immunoprecipitation experiments. This work was supported by NIH NIGMS grant GM131826.

Conflicts of interest

The author(s) declare no conflict of interest.

Literature cited

Amigoni L, Colombo S, Belotti F, Alberghina L, Martegani E. The transcription factor Swi4 is target for PKA regulation of cell size at the G_1 to S transition in *Saccharomyces cerevisiae*. Cell Cycle. 2015; 14(15):2429–2438. doi:10.1080/15384101.2015.1055997.

Amon A, Tyers M, Futcher B, Nasmyth K. Mechanisms that help the yeast cell cycle clock tick: G2 cyclins transcriptionally activate G2 cyclins and repress G1 cyclins. Cell. 1993;74(6):993–1007. doi:10.1016/0092-8674(93)90722-3.

Asa SL. The current histologic classification of thyroid cancer. Endocrinol Metab Clin North Am. 2019;48(1):1–22. doi:10.1016/j.ecl.2018.10.001.

Asadullah, Kumar S, Saxena N, Sarkar M, Barai A, Sen S. Combined heterogeneity in cell size and deformability promotes cancer invasiveness. J Cell Sci. 2021;134(7):jcs250225. doi:10.1242/jcs.250225.

Baroni MD, Martegani E, Monti P, Alberghina L. Cell size modulation by CDC25 and RAS2 genes in *Saccharomyces cerevisiae*. Mol Cell Biol. 1989;9(6):2715–2723. doi:10.1128/mcb.9.6.2715-2723.1989.

Baroni MD, Monti P, Alberghina L. Repression of growth-regulated Gl cyclin expression by cyclic AMP in budding yeast. Nature. 1994; 371(6495):339–342. doi:10.1038/371339a0.

Bhaduri S, Valk E, Winters MJ, Gruessner B, Loog M, Pryciak PM. A docking interface in the cyclin Cln2 promotes multi-site phosphorylation of substrates and timely cell-cycle entry. Curr Biol. 2015;25(3):316–325. doi:10.1016/j.cub.2014.11.069.

Brimo F, Montironi R, Egevad L, Erbersdobler A, Lin DW, Nelson JB, Rubin MA, van der Kwast T, Amin M, Epstein JI. Contemporary grading for prostate cancer: implications for patient care. Eur Urol. 2013;63(5):892–901. doi:10.1016/j.eururo.2012.10.015.

Broek D, Toda T, Michaeli T, Levin L, Birchmeier C, Zoller M, Powers S, Wigler M. The *S. cerevisiae* Cdc25 gene product regulates the Ras/adenylate cyclase pathway. Cell Press. 1987;48(5):789–799. doi:10.1016/0092-8674(87)90076-6.

Cai Y, Futcher B. Effects of the yeast RNA-binding protein Whi3 on the half-life and abundance of CLN3 mRNA and other targets, . PLoS One. 2013;8(12):e84630. doi:10.1371/journal.pone.0084630.

Cazzanelli G, Pereira F, Alves S, Francisco R, Azevedo L, Dias Carvalho P, Almeida A, Côrte-Real M, Oliveira M, Lucas C, *et al.* The yeast *Saccharomyces cerevisiae* as a model for understanding RAS proteins and their role in human tumorigenesis. Cells. 2018;7(2):14. doi:10.3390/cells7020014.

Coleman ML, Marshall CJ, Olson MF. Ras and Rho GTPases in G1-phase cell-cycle regulation. Nat Rev Mol Cell Biol. 2004;5(5): 355–366. doi:10.1038/nrm1365.

Costanzo M, Nishikawa JL, Tang X, Millman JS, Schub O, Breitkreuz K, Dewar D, Rupes I, Andrews B, Tyers M. CDK activity antagonizes Whi5, an inhibitor of G1/S transcription in yeast. Cell. 2004;117(7): 899–913. doi:10.1016/j.cell.2004.05.024.

Cross FR. DAFJ, a mutant gene affecting size control, pheromone arrest, and cell cycle kinetics of *Saccharomyces cerevisiae*. Mol Cell Biol. 1988;8(11):4675–4684. doi:10.1128/mcb.8.11.4675-4684.1988.

Cross FR, Tinkelenberg AH. A potential positive feedback loop controlling CLN1 and CLN2 gene expression at the start of the yeast cell cycle. Cell. 1991;65:875–883. doi:10.1016/0092-8674(91)903.

de Bruin RAM, McDonald WH, Kalashnikova TI, Yates J, Wittenberg C. Cln3 activates G1-specific transcription via phosphorylation of the SBF bound repressor Whi5. Cell. 2004;117(7):887–898. doi: 10.1016/j.cell.2004.05.025.

Dirick L, Böhm T, Nasmyth K. Roles and regulation of Cln-Cdc28 kinases at the start of the cell cycle of *Saccharomyces cerevisiae*. EMBO J. 1995; 14(19):4803–4813. doi:10.1002/j.1460-2075.1995.tb00162.x.

Garí E, Volpe T, Wang H, Gallego C, Futcher B, Aldea M. Whi3 binds the mRNA of the G_1 cyclin *CLN3* to modulate cell fate in budding yeast. Genes Dev. 2001;15(21):2803–2808. doi:10.1101/gad.203501.

Gothwal M, Nalwa A, Singh P, Yadav G, Bhati M, Samriya N. Role of cervical cancer biomarkers p16 and Ki67 in abnormal cervical cytological smear. J Obstet Gynecol India. 2021;71(1):72–77. doi: 10.1007/s13224-020-01380-y.

Guerra P, Vuillemenot L-APE, van Oppen YB, Been M, Milias-Argeitis A. TORC1 and PKA activity towards ribosome biogenesis oscillates in synchrony with the budding yeast cell cycle. J Cell Sci. 2022;135(18):jcs260378. doi:10.1242/jcs.260378.

Hall DD. Regulation of the Cln3-Cdc28 kinase by cAMP in *Saccharomyces cerevisiae*. EMBO J. 1998;17(15):4370–4378. doi:10.1093/emboj/17.15.4370.

Harvey SL, Enciso G, Dephoure N, Gygi SP, Gunawardena J, Kellogg DR. A phosphatase threshold sets the level of Cdk1 activity in early mitosis in budding yeast. Mol Biol Cell. 2011;22(19): 3595–3608. doi:10.1091/mbc.e11-04-0340.

Hobbs GA, Der CJ, Rossman KL. RAS isoforms and mutations in cancer at a glance. J Cell Sci. 2016;129(7):1287–1292. doi:10.1242/jcs.182873.

Hoda RS, Lu R, Arpin RN, Rosenbaum MW, Pitman MB. Risk of malignancy in pancreatic cysts with cytology of high-grade epithelial atypia. Cancer Cytopathol. 2018;126(9):773–781. doi:10.1002/cncy.22035.

Hubler L, Bradshaw-Rouse J, Heideman W. Connections between the Ras-cyclic AMP pathway and G1 cyclin expression in the budding yeast *Saccharomyces cerevisiae*. Mol Cell Biol. 1993;13(10): 6274–6282. doi:10.1128/MCB.13.10.6274.

Janke C, Magiera MM, Rathfelder N, Taxis C, Reber S, et al. A versatile toolbox for PCR-based tagging of yeast genes: new fluorescent proteins, more markers and promoter substitution cassettes. Yeast. 2004;21:947–962. doi:10.1002/ yea.1142.

Jorgensen P, Nishikawa JL, Breitkreutz B-J, Tyers M. Systematic identification of pathways that couple cell growth and division in yeast. Science. 2002;297(5580):395–400. doi:10.1126/science.1070850.

Jorgensen P, Tyers M. How cells coordinate growth and division. Curr Biol. 2004;14(23):R1014–R1027. doi:10.1016/j.cub.2004.11.027.

Kellogg DR, Levin PA. Nutrient availability as an arbiter of cell size. Trends Cell Biol. 2022;32(11):908–919. doi:10.1016/j.tcb.2022.06.008.

Kellogg DR, Murray AW. NAP1 acts with Clb2 to perform mitotic functions and to suppress polar bud growth in budding yeast. J Cell Biol. 1991;130:675–685. doi:10.1083/jcb.130.3.675.

Kerkhoff E, Rapp UR. Cell cycle targets of Ras/Raf signalling. Oncogene. 1998;17(11):1457–1462. doi:10.1038/sj.onc.1202185.

Kõivomägi M, Swaffer MP, Turner JJ, Marinov G, Skotheim JM. G_1 cyclin–Cdk promotes cell cycle entry through localized phosphorylation of RNA polymerase II. Science. 2021;374(6565):347–351. doi:10.1126/science.aba5186.

Landry BD, Doyle JP, Toczyski DP, Benanti JA. F-box protein specificity for G1 cyclins is dictated by subcellular localization. PLoS Genet. 2012;8(7):e1002851. doi:10.1371/journal.pgen.1002851.

Litsios A, Goswami P, Terpstra HM, Coffin C, Vuillemenot L-A, Rovetta M, Ghazal G, Guerra P, Buczak K, Schmidt A, *et al.* The timing of start is determined primarily by increased synthesis of the Cln3 activator rather than dilution of the Whi5 inhibitor. Mol Biol Cell. 2022;33(5):rp2. doi:10.1091/mbc.E21-07-0349.

Litsios A, Huberts DHEW, Terpstra HM, Guerra P, Schmidt A, Buczak K, Papagiannakis A, Rovetta M, Hekelaar J, Hubmann G, *et al.* Differential scaling between G1 protein production and cell size dynamics promotes commitment to the cell division cycle in budding yeast. Nat Cell Biol. 2019;21(11):1382–1392. doi:10.1038/s41556-019-0413-3.

Liu S, Tan C, Tyers M, Zetterberg A, Kafri R. What programs the size of animal cells? Front. Cell Dev Biol. 2022;10:949382. doi:10.3389/fcell.2022.949382.

Longtine MS, McKenzie A, DeMarini DJ, Shah NG, Wach A, et al. Additional modules for versatile and eco- nomical PCR-based gene deletion and modification in *Saccharomyces cerevisiae*. Yeast. 1998;14:953–961. doi:10.1002/(SICI)1097-0061(199807)14:10,953::AID-YEA293.3.0.CO;2-U.

Lucena R, Alcaide-Gavilán M, Schubert K, He M, Domnauer MG, Marquer C, Klose C, Surma MA, Kellogg DR. Cell size and growth rate are modulated by TORC2-dependent signals. Curr Biol. 2018;28(2):196–210.e4. doi:10.1016/j.cub.2017.11.069.

Matsumoto K, Uno I, Ishikawa T. Control of cell division in *Saccharomyces cerevisiae* mutants defective in adenylate cyclase and cAMP-dependent protein kinase. Exp Cell Res. 1983;146(1):151–161. doi:10.1016/0014-4827(83)90333-6.

Mizunuma M, Tsubakiyama R, Ogawa T, Shitamukai A, Kobayashi Y, Inai T, Kume K, Hirata D. Ras/cAMP-dependent protein kinase (PKA) regulates multiple aspects of cellular events by phosphorylating the Whi3 cell cycle regulator in budding yeast. J Biol Chem. 2013;288(15):10558–10566. doi:10.1074/jbc.M112.402214.

Morishita T, Mitsuzawa H, Nakafuku M, Nakamura S, Hattori S, Anraku Y. Requirement of *Saccharomyces cerevisiae* Ras for completion of mitosis. Science. 1995;270(5239):1213–1215. doi:10.1126/science.270.5239.1213.

Muise-Helmericks RC, Grimes HL, Bellacosa A, Malstrom SE, Tsichlis PN, Rosen N. Cyclin D expression is controlled post-transcriptionally via a phosphatidylinositol 3-kinase/Akt-dependent pathway. J Biol Chem. 1998;273(45):29864–29872. doi:10.1074/jbc.273.45.29864.

Nash R, Tokiwa G, Anand S, Erickson K, Futcher AB. The WHI1 + gene of *Saccharomyces cerevisiae* tethers cell division to cell size and is a cyclin homolog. EMBO J. 1988;7(13):4335–4346. doi:10.1002/j.1460-2075.1988.tb03332.x.

Nash RS, Volpe T, Futcher B. Isolation and characterization of WHI3, a size-control gene of *Saccharomyces cerevisiae*. Genetics. 2001;157(4):1469–1480. doi:10.1093/genetics/157.4.1469.

Nasmyth K, Dirick L. The role of SW4 and SW16 in the activity of Gl cyclins in yeast. Cell. 1991;66(5):995–1013. doi:10.1016/0092-8674(91)90444-4.

Ottoz DSM, Rudolf F, Stelling J. Inducible, tightly regulated and growth condition-independent transcription factor in *Saccharomyces cerevisiae*. Nucleic Acids Res. 2014;42(17):e130. doi:10.1093/nar/gku616.

Pruitt K, Der CJ. Ras and Rho regulation of the cell cycle and oncogenesis. Cancer Lett. 2001;171(1):1–10. doi:10.1016/S0304-3835(01)00528-6.

Pruitt K, Pestell RG, Der CJ. Ras inactivation of the retinoblastoma pathway by distinct mechanisms in NIH 3T3 fibroblast and RIE-1 epithelial cells. J Biol Chem. 2000;275(52):40916–40924. doi:10.1074/jbc.M006682200.

Robinson LC, Gibbs JB, Marshall MS, Sigal IS, Tatchell K. CDC25: a component of the RAS-adenylate cyclase pathway in *Saccharomyces cerevisiae*. Science. 1987;235(4793):1218–1221. doi:10.1126/science.3547648.

Sandlin CW, Gu S, Xu J, Deshpande C, Feldman MD, Good MC. Epithelial cell size dysregulation in human lung adenocarcinoma. PLoS One. 2022;17(10):e0274091. doi:10.1371/journal.pone.0274091.

Seshan A, Amon A. Ras and the Rho effector Cla4 collaborate to target and anchor Lte1 at the bud cortex. Cell Cycle. 2005;4(7):940–946. doi:10.4161/cc.4.7.1785.

Sommer RA, DeWitt JT, Tan R, Kellogg DR. Growth-dependent signals drive an increase in early G1 cyclin concentration to link cell cycle entry with cell growth. eLife. 2021;10:e64364. doi:10.7554/eLife.64364.

Stuart D, Wittenberg C. CLN3, not positive feedback, determines the timing of CLN2 transcription in cycling cells. Genes Dev. 1995;9(22):2780–2794. doi:10.1101/gad.9.22.2780.

Tatchell K, Robinson LC, Breitenbach M. RAS2 of *Saccharomyces cerevisiae* is required for gluconeogenic growth and proper response to nutrient limitation. Proc Natl Acad Sci USA. 1985;82(11):3785–3789. doi:10.1073/pnas.82.11.3785.

Toda T, Cameron S, Sass P, Zoller M, Scott JD, Mcmullen B, Hurwitz M, Krebs EG, Wigler M. Cloning and characterization of BCY1, a locus encoding a regulatory subunit of the cyclic AMP-dependent protein kinase in *Saccharomyces cerevisiae*. Mol Cell Biol. 1987;7(4):1371–1377. doi:10.1128/mcb.7.4.1371-1377.1987.

Toda T, Uno I, Ishikawa T, Powers S, Kataoka T, Broek D, Cameron S, Broach J, Matsumoto K, Wigler M. In yeast, RAS proteins are controlling elements of adenylate cyclase. Cell. 1985;40(1):27–36. doi:10.1016/0092-8674(85)90305-8.

Tokiwa G, Tyers M, Volpe T, Futcher B. Inhibition of G1 cyclin activity by the Ras/cAMP pathway in yeast. Nature. 1994;371(6495):342–345. doi:10.1038/371342a0.

Turner JJ, Ewald JC, Skotheim JM. Cell size control in yeast. Curr Biol. 2012;22(9):R350–R359. doi:10.1016/j.cub.2012.02.041.

Tyers M, Tokiwa G, Futcher B. Comparison of the *Saccharomyces cerevisiae* G1 cyclins: Cln3 may be an upstream activator of Cln1, Cln2 and other cyclins. EMBO J. 1993;12(5):1955–1968. doi:10.1002/j.1460-2075.1993.tb05845.x.

Wang H, Carey LB, Cai Y, Wijnen H, Futcher B. Recruitment of Cln3 cyclin to promoters controls cell cycle entry via histone deacetylase and other targets. PLoS Biol. 2009;7(9):e1000189. doi:10.1371/journal.pbio.1000189.

Wang H, Garí E, Vergés E, Gallego C, Aldea M. Recruitment of Cdc28 by Whi3 restricts nuclear accumulation of the G1 cyclin–Cdk complex to late G1. EMBO J. 2004;23(1):180–190. doi:10.1038/sj.emboj.7600022.

Weiss RA. A perspective on the early days of RAS research. Cancer Metastasis Rev. 2020;39(4):1023–1028. doi:10.1007/s10555-020-09919-1.

Zaman S, Lippman SI, Schneper L, Slonim N, Broach JR. Glucose regulates transcription in yeast through a network of signaling pathways. Mol Syst Biol. 2009;5(1):245. doi:10.1038/msb.2009.2.

Zamora-Domínguez JA, Olarte-Carrillo I, Ruiz-Ramos R, Ramos-Peñafiel C, Jiménez-Zamudio LA, García Latorre E, Centeno Cruz F, Martínez Tovar A. Abnormal expression of *H-Ras* induces S-phase arrest and mitotic catastrophe in human T-lymphocyte leukemia. Blood Res. 2023;58(1):20–27. doi:10.5045/br.2023.2022143.

Zapata J, Dephoure N, MacDonough T, Yu Y, Parnell EJ, Mooring M, Gygi SP, Stillman DJ, Kellogg DR. PP2ARts1 is a master regulator of pathways that control cell size. J Cell Biol. 2014;204(3):359–376. doi:10.1083/jcb.201309119.

Editor: A. Gladfelter